iScience

CellPress
OPEN ACCESS

Article

Adipose-mesenchymal stromal cells suppress experimental Sjögren syndrome by IL-33-driven expansion of ST2^{+} regulatory T cells

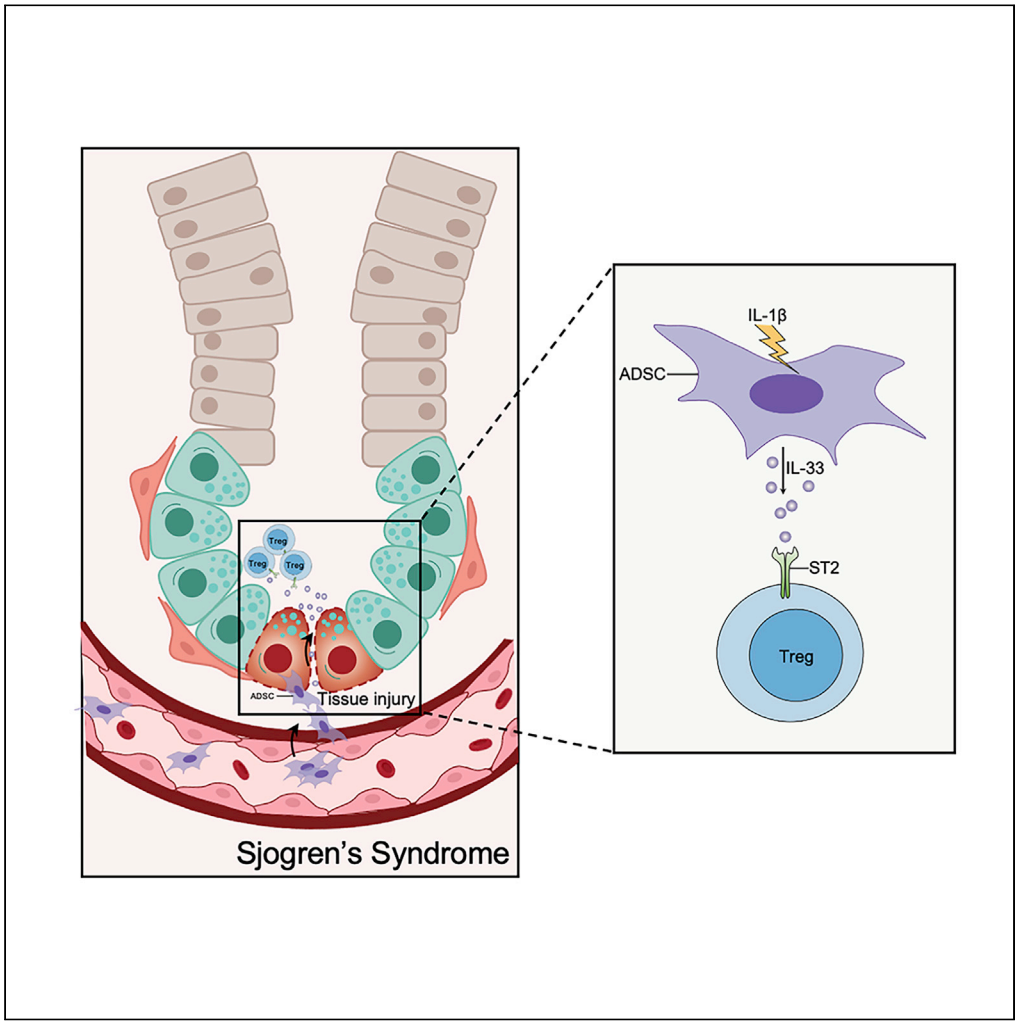

Ousheng Liu, Junji Xu, Fu Wang, ..., Songlin Wang, Zhangui Tang, Wanjun Chen

wchen@dir.nidcr.nih.gov

Highlights

Human and mouse ADSCs express IL-33 in response to IL-β stimulation

mADSC-derived IL-33 inhibits inflammation in salivary glands in SS model

mADSC-derived IL-33 expand ST2^{+} Tregs *in vitro* and in SS model

Liu et al., iScience *24*, 102446
May 21, 2021
https://doi.org/10.1016/j.isci.2021.102446

iScience

CellPress
OPEN ACCESS

Article

Adipose-mesenchymal stromal cells suppress experimental Sjögren syndrome by IL-33-driven expansion of ST2$^+$ regulatory T cells

Ousheng Liu,[1,2] Junji Xu,[1] Fu Wang,[1,3] Wenwen Jin,[1] Peter Zanvit,[1] Dandan Wang,[1] Nathan Goldberg,[1] Alexander Cain,[1] Nancy Guo,[1] Yichen Han,[1] Andrew Bynum,[1] Guowu Ma,[3] Songlin Wang,[4] Zhangui Tang,[2] and Wanjun Chen[1,5,*]

SUMMARY

Adipose-derived mesenchymal stromal cells (ADSCs) play important roles in the alleviation of inflammation and autoimmune diseases. Interleukin-33 (IL-33), a member of the IL-1 family, has been shown to regulate innate and adaptive immunity. However, it is still unknown whether ADSCs regulate immune responses via IL-33. We show here that ADSCs produced IL-33 in response to IL-1β stimulation, which depended on TAK1, ERK, and p38 pathways. ADSCs-derived IL-33 drove the proliferation of CD4$^+$Foxp3$^+$ST2$^+$ regulatory T cells (Tregs) and alleviated experimental autoimmune Sjögren syndrome in mice. Importantly, human ADSCs also produced IL-33 in response to IL-1β. Thus, we have revealed a previously unrecognized immunoregulatory function of ADSCs by IL-33 production in experimental autoimmunity, which may have clinical applications for human immunopathology.

INTRODUCTION

Adipose-derived mesenchymal stromal cells (ADSCs), a subtype of mesenchymal stromal cells (MSCs), played important roles in regenerative medicine to differentiating in bone and adipocytes and in modulating immune responses and alleviating inflammation or autoimmune diseases including arthritis, colitis, and autoimmune diabetes (Bassi et al., 2012; Gonzalez et al., 2009a, 2009b; Mizuno et al., 2012; Razmkhah et al., 2015; Shang et al., 2015; Zuk et al., 2001). The MSCs-tracking analysis showed that exogenously delivered MSCs could be detected in inflamed zones for the first week after injection, suggesting their interaction with inflammatory cells and cytokines. Indeed, studies reported that inflammatory cytokines such as interferon (IFN)-γ, interleukin (IL)-1β, and tumor necrosis factor (TNF)-α could be critical for MSC-mediated immunoregulation (Castelo-Branco et al., 2012; Chen et al., 2013; Tanaka et al., 2008; Xu et al., 2012). The inflammatory cytokines drive the immunosuppression function of MSCs through expression and release of different factors and cytokines in the inflammatory "niches" (Krampera et al., 2006; Meisel et al., 2004; Mougiakakos et al., 2011; Ren et al., 2008, 2009; Sheng et al., 2008).

IL-33 was first reported as a novel member of the IL-1 family in 2005 (Schmitz et al., 2005) and is now recognized as a crucial factor in influencing innate and adaptive immunity (Ali et al., 2011). Among its pleiotropic functions (Baumann et al., 2015; Gao et al., 2015; Hepworth et al., 2012; Price et al., 2010; Reichenbach et al., 2015; Yang et al., 2011), IL-33 drives proliferation of CD4$^+$Foxp3$^+$ regulatory T cells (Tregs) and group 2 innate lymphoid cells (ILC2s) and regulates immune responses in lymphoid organs, gut, lungs, and adipose tissues (Arpaia et al., 2015; Matta et al., 2016; Molofsky et al., 2015b; Mougiakakos et al., 2011; Schiering et al., 2014). IL-33 also functions for the maintenance of tissue homeostasis and repair of tissue damage (Liew et al., 2016; Molofsky et al., 2015a). Typically IL-33 is expressed at high levels in the nuclei of various cell types in human and mouse tissues in the steady state, including endothelial cells (Chen et al., 2015), epithelial cells (Nakanishi et al., 2013), macrophages, and fibroblast-like cells (Moussion et al., 2008; Pichery et al., 2012). Besides, it was recently reported that some subsets of MSCs expressing IL-33 were involved in the homeostasis and metabolism of adipocytes (Mahlakoiv et al., 2019). However, it remains largely unknown what drives MSCs to produce IL-33 and whether the IL-33 has immunoregulatory effects on distant organs and tissues beyond adipose tissues.

[1]Mucosal Immunology Section, NIDCR, NIH, Bethesda, MD 20892, USA

[2]Hunan Key Laboratory of Oral Health Research & Hunan 3D Printing Engineering Research Center of Oral Care & Hunan Clinical Research Center of Oral Major Diseases and Oral Health & Xiangya Stomatological Hospital & Xiangya School of Stomatology, Central South University, Changsha 410008, China

[3]Dalian Medical University, School of Stomatology, Dalian 116044, China

[4]Molecular Laboratory for Gene Therapy and Tooth Regeneration, Beijing Key Laboratory of Tooth Regeneration and Function Reconstruction, School of Stomatology, Capital Medical University, Beijing 100050, China

[5]Lead contact

*Correspondence: wchen@dir.nidcr.nih.gov

https://doi.org/10.1016/j.isci.2021.102446

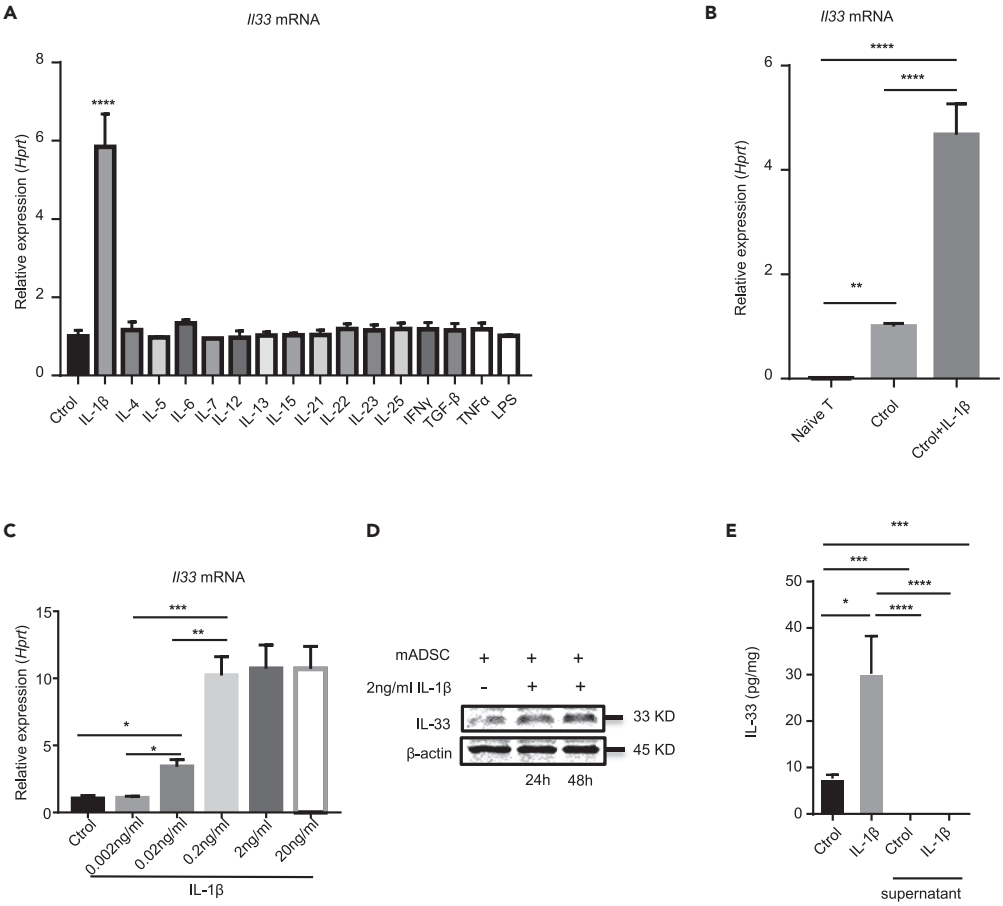

Figure 1. mADSC can produce IL-33 with IL-1β stimulation

(A) *Il33* mRNA expression in mADSC stimulated for 6 h with different cytokines as indicated. (2 ng/mL IL-1β, 10 ng/mL IL-4, 10 ng/mL IL-5, 50 ng/mL IL-6, 10 ng/mL IL-7, 10 ng/mL IL-12, 10 ng/mL IL-13, 10 ng/mL IL-15, 10 ng/mL IL-21, 10 ng/mL IL-22, 10 ng/mL IL-23, 10 ng/mL IL-25,10 ng/mL IFNγ, 2 ng/mL TGF-β, 10 ng/mL TNFα, 10 ng/mL LPS).

(B) *Il33* mRNA can be produced in mADSC stimulated for 6 h with 10 ng/mL IL-1β.

(C) *Il33* mRNA in mADSC stimulated for 6 h with different dose of concentration of IL-1β (0, 0.002, 0.02, 0.2, 2 and 20 ng/mL).

(D) Western blot of IL-33 and β-actin in mADSC stimulated with or without 2 ng/mL IL-1β for 24 or 48 h

(E) ELISA of IL-33 in mADSC lysate and supernatant stimulated with or without 10 ng/mL IL-1β for 72 h. Data are pooled from three (A and C) independent experiments or are representative of three (B, D, and E) independent experiments. In (A), (B), (C), and (E) one-way ANOVA was used. Bars, mean; error bars, SEM; *$p < 0.05$, **$p < 0.01$, ***$p < 0.001$, ****$p < 0.0001$.

RESULTS

Murine ADSCs produce IL-33 in response to IL-1β

ADSCs from C57BL/6 mice and IL-33-deficient mice (C57BL/6J-*Il33*$^{tm1b(EUCOMM)Cln}$, *Il33*$^{-/-}$) were isolated from subcutaneous fat tissues. ADSCs were determined based on their positivity for MSC markers SCA-1, CD44, CD90, and CD105 and negativity for epithelial cell marker CD31 and hematopoietic cell marker CD45 (Bourin et al., 2013) (Figure S1A). Also, ADSCs were functionally capable of differentiating into adipocytes, osteoblasts, and chondroblasts under standard differentiation culture conditions (Figure S1B). ADSCs exhibited no difference in their surface markers and multiple differentiation potential from wild-type (WT) and *Il33*$^{-/-}$ mice.

To mimic IL-33 production from mADSCs in the inflammatory "niches," we stimulated ADSCs that were isolated from C57BL/6 mice with a panel of inflammatory cytokines in cultures for 6 h *Il33* mRNA was determined by real-time PCR. Among the comprehensive panel of the cytokines we examined, only IL-1β was able to significantly upregulate *Il33* mRNA expression in ADSCs (Figure 1A). ADSCs expressed

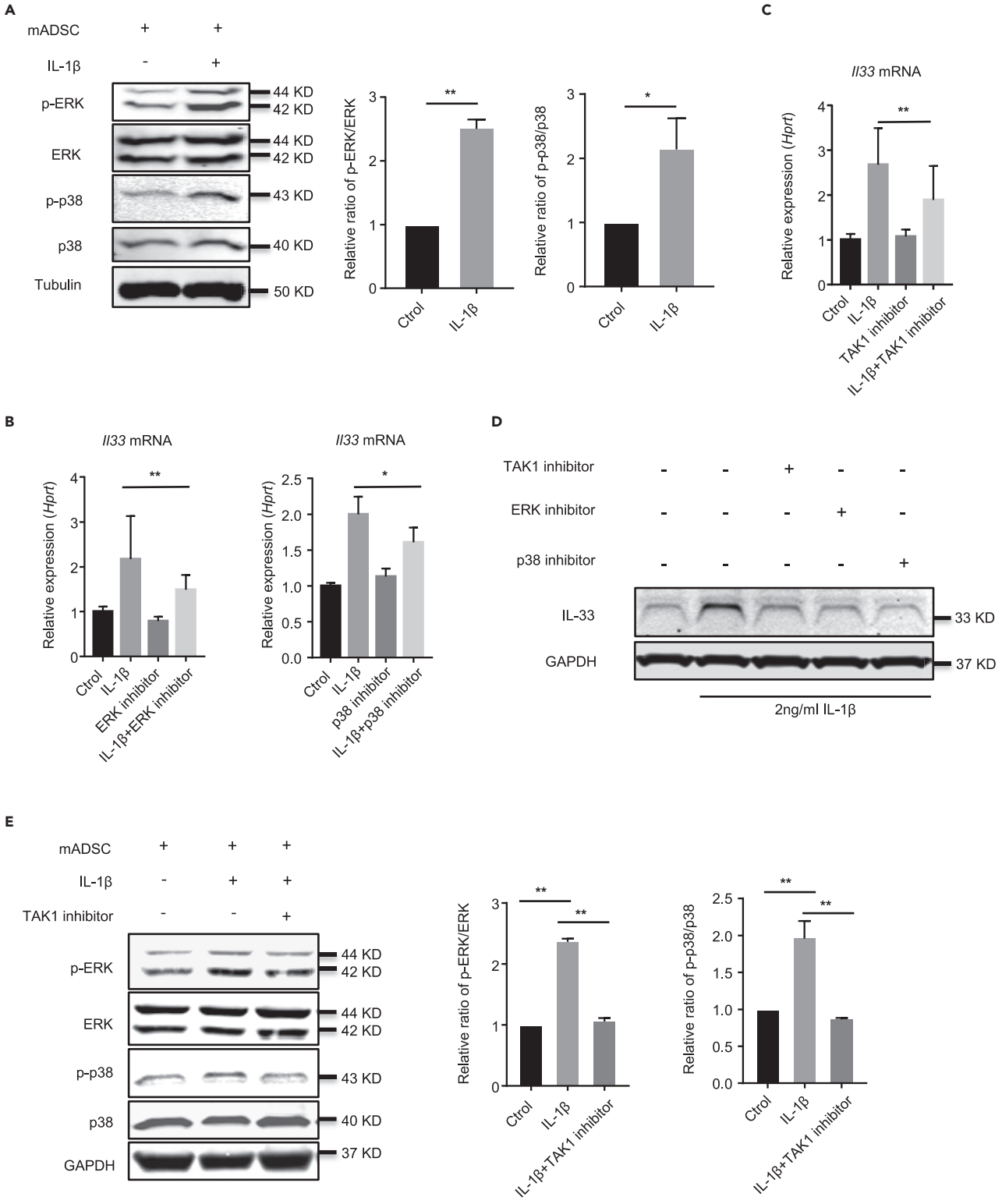

Figure 2. IL-1β upregulates IL-33 expression by promoting TAK1, ERK, and p38 pathway in mADSC

(A) Western blot of p-ERK, ERK, p-p38, p38, and Tubulin in mADSC stimulated with or without IL-1β for 2 h

(B) *Il33* mRNA expression in mADSC stimulated with or without IL-1β, ERK inhibitor, or p38 inhibitor for 6 h

(C) *Il33* mRNA expression in mADSC stimulated with or without IL-1β, TAK1 inhibitor for 6 h.

Figure 2. *Continued*

(D) Western blot of IL-33 and GAPDH in mADSC stimulated with or without IL-1β, TAK1 inhibitor, ERK inhibitor, or p38 inhibitor for 24 h.

(E) Western blot of p-ERK, ERK, p-p38, p38, and GAPDH in mADSC stimulated with or without IL-1β, TAK1 inhibitor for 1 h. Data are pooled from three (B and C) independent experiments or are representative of three (A, D, and E) independent experiments. In (A), Student's t test was used. In (B), (C), and (E) one-way ANOVA was used. Bars, mean; error bars, SEM; *p < 0.05, **p < 0.01.

spontaneous base levels of *Il33* mRNA higher than did T cells (Figure 1B). IL-1β driving *Il33* mRNA expression in ADSCs was dose-dependent and reached a plateau at 0.2 ng/mL of IL-1β (Figure 1C). Consistent with *Il33* mRNA, western blot analysis showed a substantially higher level of IL-33 protein in IL-1β-treated ADSCs compared with untreated cells (Figure 1D). ELISA analysis also showed higher levels of IL-33 protein in the cell lysates from IL-1β-treated ADSCs when compared with the untreated cells, although IL-33 was hardly detected in the cell culture supernatants from all the cultures (Figure 1E). Of note, although IFN-γ alone was unable to induce *Il33* mRNA, it enhanced IL-β-induced IL-33 in mouse ADSCs (Figure S2). Thus, mADSCs produce IL-33 upon IL-1β stimulation.

IL-1β upregulates IL-33 through TAK1-ERK/p38 pathways in mADSCs

We next investigated the signaling pathways by which IL-33 was induced by IL-1β stimulation in ADSCs. We first analyzed the expression and activation of ERK, p38, JNK, and nuclear factor (NF)-κB proteins in ADSCs stimulated with IL-1β. We found that the relative ratio of phosphorylated ERK (p-ERK)/ERK and phosphorylated p38 (p-p38)/p38 were increased in ADSCs treated with IL-1β compared with the untreated cells (Figure 2A). However, there were no significant differences between the phosphorylated JNK and NF-κB (p65) proteins between IL-1β-treated and untreated ADSCs (Figures S3A and S3B).

Next, we investigated which of the aforementioned pathways was involved in IL-1β-driven IL-33 induction in ADSCs by utilizing the selective protein kinase inhibitors 0.2 μM U0126 (for ERK), 20 μM SB203580 (for p38 MAPK), 2 μM SP600125 (for JNK), and 2 μM JSH23 (for NF-κB) to block the activity of the indicated proteins. We found that inhibition of ERK and p38 MAPK activity significantly reduced IL-1β-induced *Il33* mRNA and IL-33 protein (Figures 2B and 2D), whereas inhibition of JNK and NF-κB failed to do so (Figures S3C and S3D). In addition, suppression of TAK1 activity also decreased *Il33* mRNA and IL-33 protein in ADSCs (Figures 2C and 2D). To explore the mechanism of the TAK1 signal pathway during IL-1β-driven IL-33, we examined whether TAK1 inhibition affects the phosphorylation of p38 and ERK. Our result showed that the phosphorylation of p38 and ERK was significantly reduced in TAK1 inhibitor (100 nM) group after IL-1β treatment (Figure 2E). These data suggest that IL-1β activates TAK1, up-regulating phosphorylation of p38 and ERK, and subsequently mediates IL-33 expression.

mADSCs-derived IL-33 regulates ST2 expression in Tregs *in vitro*

To determine the immunoregulatory function of IL-33 produced by ADSCs, we next studied the effects of IL-1β-treated mADSCs lysates on $CD4^+CD25^+Foxp3^+$ Tregs (Chen et al., 2003), because IL-33 has been shown to promote the proliferation of Tregs (Matta et al., 2016; Vasanthakumar et al., 2015). ADSCs from WT or $Il33^{-/-}$ mice were cultured with or without IL-1β to confirm that *Il33* mRNA and IL-33 protein were detected only in WT but not $Il33^{-/-}$ cells (Figures 3A and 3B). $CD4^+CD25^+$ Tregs isolated from spleen and lymph nodes in C57BL/6 mice were cultured with IL-1β-stimulated WT or $Il33^{-/-}$ ADSCs lysates. We found that IL-1β-stimulated WT ADSCs lysates significantly upregulated *Il1rl1* mRNA (receptor for IL-33, ST2) expression in Tregs, which was abrogated by the inclusion of anti-IL-33 antibody in the cultures (Figure 3C). Consistently, IL-1β-stimulated $Il33^{-/-}$ ADSCs lysates exhibited significantly lower activity to upregulate *Il1rl1* mRNA in Tregs than did WT ADSCs lysates (Figure 3C). Consequently, the frequency and the absolute number of $ST2^+$ Treg subsets within the $CD4^+Foxp3^+$ Tregs cultured with IL-1β-treated WT ADSCs were much higher than those of $ST2^+$ Treg subsets in Tregs treated with $Il33^{-/-}$ ADSCs (Figures 3D and 3E). Consistently, the increase in $ST2^+$ Tregs in Tregs stimulated with WT ADSCs was entirely abolished by neutralization of IL-33 with anti-IL33 antibody (Figure 3E). The data collectively indicate that IL-33 from mADSCs upregulates $ST2^+$ Tregs in cultures.

WT but not $Il33^{-/-}$ mADSCs improve Sjögren syndrome by suppressing inflammation in salivary glands in NOD mice

The expansion of $ST2^+$ Tregs by ADSCs-derived IL-33 encouraged us to investigate the immunoregulatory and therapeutic function of ADSCs in autoimmunity and inflammation *in vivo*. For this, we intravenously injected WT and $Il33^{-/-}$ mADSCs (both on C57BL/6 background) into allogeneic NOD/ShiLtj mice (NOD, on

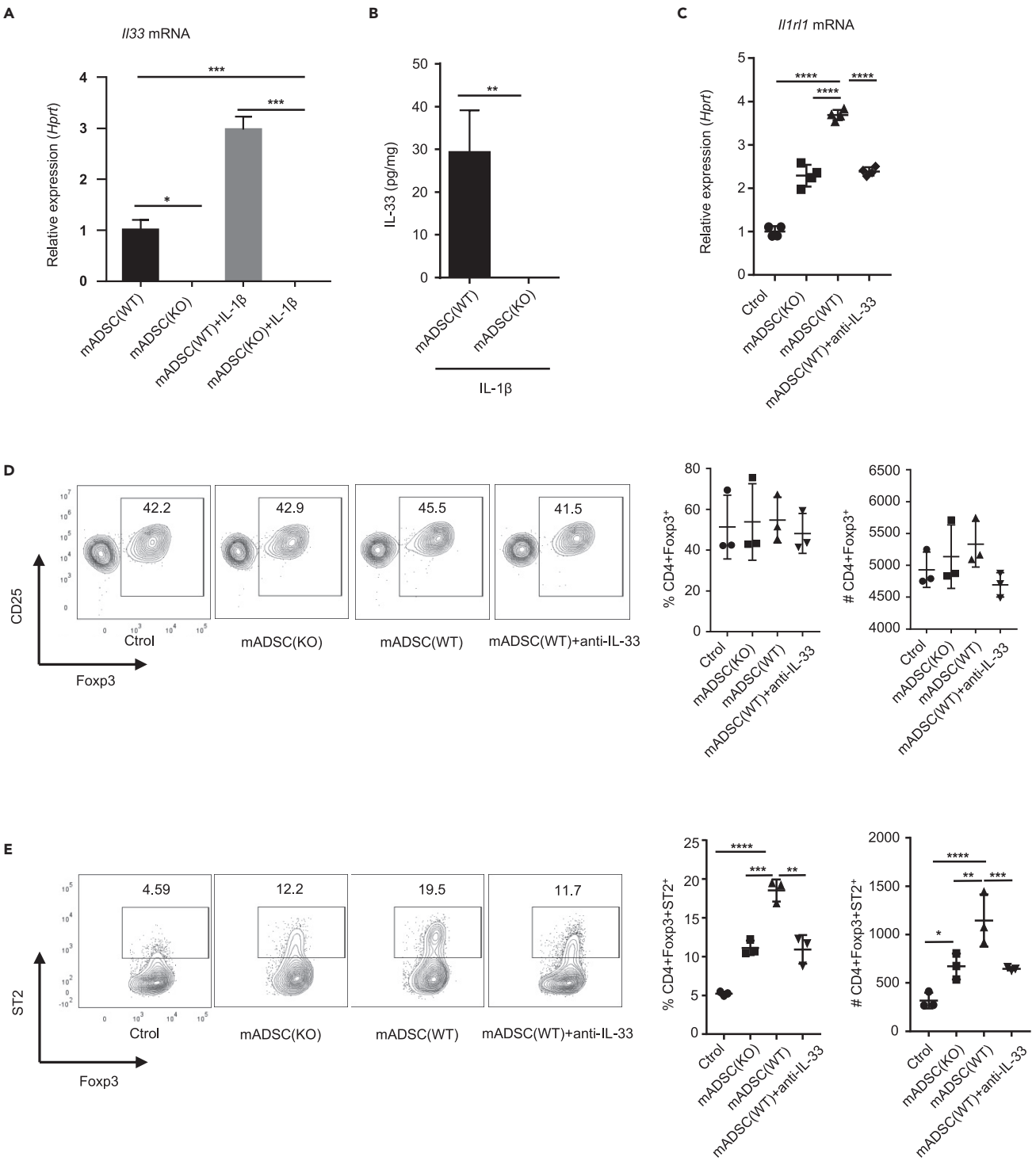

Figure 3. IL-33 from mADSC affects ST2 expression on Treg *in vitro*

(A) *Il33* mRNA expression in ADSC from WT and *Il33*$^{-/-}$ mice stimulated for 6 h with or without 10 ng/mL IL-1β.

(B) ELISA of IL-33 protein in mADSC stimulated with 10 ng/mL IL-1β for 72 h

(C) *Il1rl1* mRNA expression in CD4^{+}CD25^{+} T cell from spleen with anti-CD3/CD28 plus stimulated with or without ADSC lysate from WT or *Il33*$^{-/-}$ mice or ADSC soap from WT mice with anti-IL-33 for 24 h.

(D) Frequency and absolute number of Foxp3^{+} T cells in CD4^{+}CD25^{+} T cell from spleen with anti-CD3/CD28 plus stimulated with or without ADSC lysate from WT or *Il33*$^{-/-}$ mice or ADSC soap from WT mice with anti-IL-33 for 72 h.

Figure 3. *Continued*

(E) Frequency and absolute number of ST2$^+$ T cells in CD4$^+$Foxp3$^+$ T cell from spleen with anti-CD3/CD28 plus stimulated with or without ADSC lysate from WT or *Il33*$^{-/-}$ mice or ADSC soap from WT mice with anti-IL33 for 72 h. Data are pooled from three (A, C, D, and E) independent experiments or are representative of three (B) independent experiments. In (B), Student's t test was used. In (A), (C), (D), and (E), one-way ANOVA was used. Bars, mean; error bars, SEM; *p < 0.05, **p < 0.01, ***p < 0.001, ****p < 0.0001.

Cataract Shionogi background) that have been well known to develop an autoimmune Sjögren syndrome (SS) spontaneously. The rationale underlying the utilization of allogeneic ADSC transplantation was based on the published animal and clinical studies that show negligible allorejection and side effects of allogeneic MSCs transplantation due to the non/low MHC II expression on MSCs, yet exhibition of beneficial and immunoregulatory function (Alexeev et al., 2014; Xu et al., 2012). We injected allogeneic ADSCs from WT or *Il33*$^{-/-}$ mice or PBS into NOD/ShiLtj mice at 7 weeks of age when the inflammation starts to occur in the submandibular glands. Yet, the secretory function of the submandibular glands has not been compromised (Delaleu et al., 2011). The saliva flow rates were measured weekly from 7 through 13 weeks (Figure S4A). We found that WT ADSCs transplantation significantly improved the saliva flow rates 2 weeks after injection in NOD/ShiLtj mice compared with PBS- or *Il33*$^{-/-}$ mADSCs-treated mice (Figure 4A). We then examined the expression of genes, including *Slc12a2*, *Tjp1*, *Aqp5*, *Itpr3*, *Trpv4*, and *Chrm3*, which have been known to be relevant to submandibular gland function at the 13th week (Markadieu and Delpire, 2014; Wang et al., 2017). The expressions of all those genes except *Aqp5* mRNA in submandibular glands were significantly increased in WT ADSCs-treated mice compared with the mice treated with *Il33*$^{-/-}$ mADSCs or PBS (Figures 4B–4G). Consistent with the improvement of saliva flow and the upregulation of the genes associated with submandibular gland function, histological analysis of the submandibular gland tissues revealed that transplantation of WT ADSCs resulted in a substantial reduction of inflammatory areas in the submandibular glands compared with *Il33*$^{-/-}$ ADSCs- or PBS-treated groups (Figures 4H and 4I). These findings altogether indicate that allogeneic ADSCs suppress inflammation and improve the secretory function of salivary glands in an IL-33-dependent manner.

ADSC-derived IL-33 upregulates ST2$^+$ Tregs in NOD mice

To understand the underlying mechanisms by which allogeneic ADSCs IL-33 suppressed inflammation and improved the function of submandibular glands, we examined the changes of Tregs and proinflammatory effector cells in the submandibular glands of NOD mice. Strikingly, WT ADSCs treatment resulted in a significant increase in both the frequency and absolute number of CD4$^+$Foxp3$^+$ Tregs in the submandibular glands in SS-like NOD mice compared with other groups (Figure 5A). More importantly, WT ADSCs treatment, but not *Il33*$^{-/-}$ ADSCs treatment, led to a significant increase in the frequency and total number of ST2$^+$ Tregs (Figure 5B). Further analysis of *in vivo* Treg expansion with Ki67 staining revealed that WT ADSCs treatment caused significantly more Ki67$^+$ Tregs in the submandibular glands than did *Il33*$^{-/-}$ ADSCs or PBS treatment, suggesting IL-33-driven Treg proliferation upon WT ADSCs transplantation (Figure 5C).

As IL-33 is also associated with the differentiation and function of various lymphocytes including type 2 helper T (Th2) cells and ILC2s (Licona-Limon et al., 2013; Molofsky et al., 2013; Moro et al., 2010; Schmitz et al., 2005) in addition to Tregs, we studied Th2 (IL-4$^+$, IL-13$^+$) CD4$^+$ T cells and ILC2s in the submandibular glands among all the groups of NOD mice and no significant differences could be observed (Figures S4–S7). Furthermore, the frequency of IL-13-expressing (Lin$^-$CD45$^+$GATA3$^+$ST2$^+$IL-13$^+$) and IL-4-producing (Lin$^-$CD45$^+$GATA3$^+$ST2$^+$IL-4$^+$) ILC2 subsets also did not exhibit changes after ADSCs treatment (Figures S8A–S8C). Interestingly, the frequency of CD8$^+$TCR$\alpha\beta^+$IL-4$^+$ T cells increased in the submandibular glands of WT ADSCs-treated group compared with *Il33*$^{-/-}$ ADSCs- or PBS-treated groups (Figure S6D), but the significance of the increase remains unknown.

We next examined the CD45$^+$ inflammatory cells in the submandibular glands. WT ADSCs treatment caused significantly fewer CD45$^+$ cells in the submandibular glands than *Il33*$^{-/-}$ ADSCs or PBS-treated mice (Figure 5D). The absolute number of CD4$^+$ (Figure 5E) and CD8$^+$ (Figure 5F) T cells, but not TCR$\gamma\delta^+$ T cells (Figure 5G), significantly decreased in WT ADSC-treated mice compared with *Il33*$^{-/-}$ ADSCs- or PBS- treated groups. Consequently, the total number of IFN-γ^+CD4$^+$ T cells (Th1) and IFN-γ^+CD8$^+$ T cells were decreased in WT ADSC-treated NOD mice, although the frequency did not change significantly (Figures S4B–S4E, S5A, S5E, S6A, S6E, S7A, and S7E). Interestingly, both WT and *Il33*$^{-/-}$ mADSCs treatment showed a similar reduction of IL-17$^+$ T cells compared with the PBS group, suggesting that

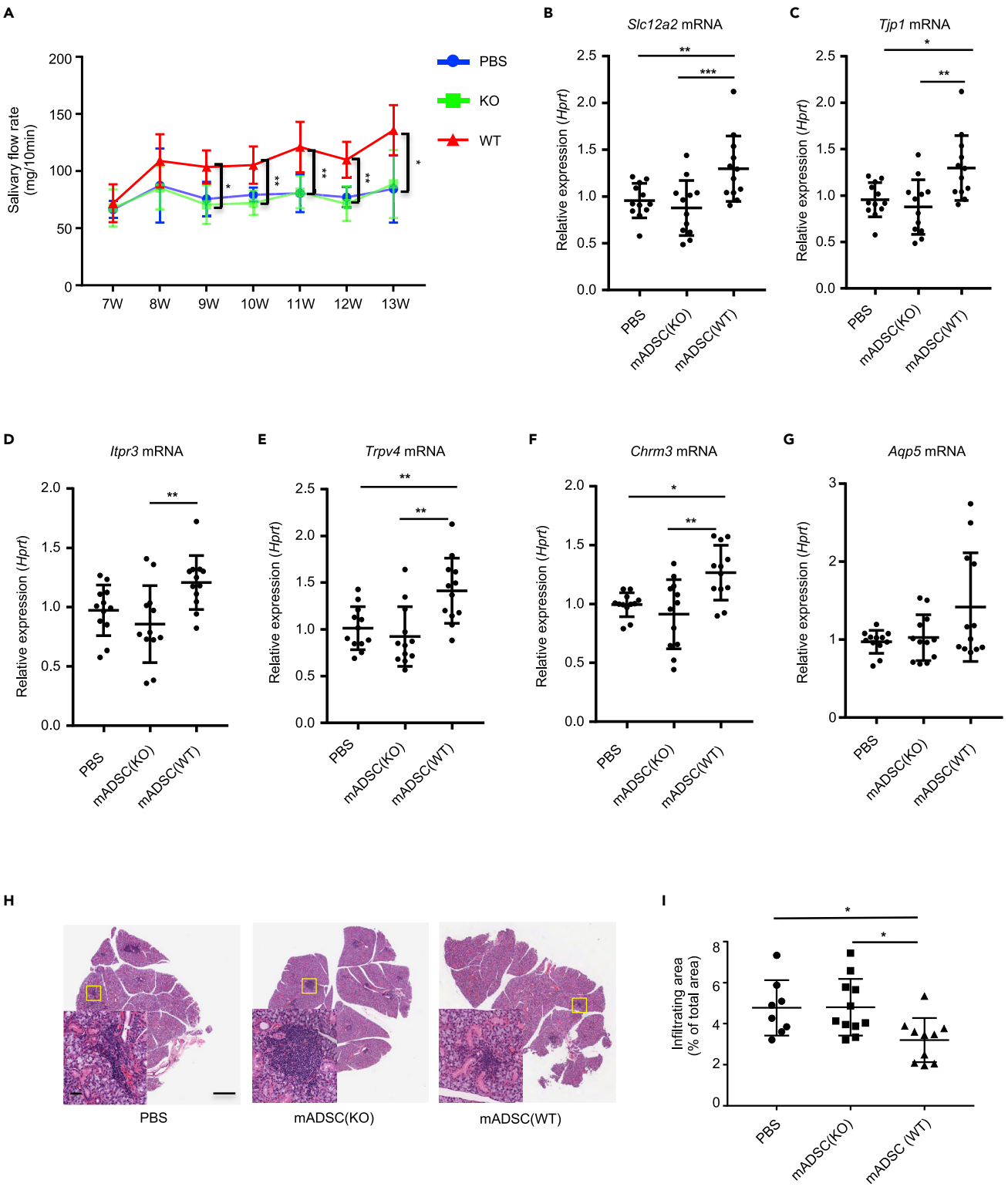

Figure 4. WT but not *Il33*$^{-/-}$ mADSCs suppress inflamed tissue damage and improve submandibular gland function in NOD/ShiLtj mice

(A) Salivary flow rate of NOD/ShiLtj treated with PBS, ADSC from WT or *Il33*$^{-/-}$ mice. PBS group (n = 12), KO group (n = 12), WT group (n = 12). (B) *Slc12a2* mRNA expression in the submandibular glands of NOD/ShiLtj mice injected with PBS, ADSC from WT or *Il33*$^{-/-}$ mice.

(C) *Tjp1* mRNA expression in the submandibular glands of NOD/ShiLtj mice injected with PBS, ADSC from WT or *Il33*$^{-/-}$ mice.

(D) *Itpr3* mRNA expression in the submandibular glands of NOD/ShiLtj mice injected with PBS, ADSC from WT or *Il33*$^{-/-}$ mice.

Figure 4. *Continued*

(E) *Trpv4* mRNA expression in the submandibular glands of NOD/ShiLtj mice injected with PBS, ADSC from WT or *Il33*$^{-/-}$ mice.
(F) *Chrm3* mRNA expression in the submandibular glands of NOD/ShiLtj mice injected with PBS, ADSC from WT or *Il33*$^{-/-}$ mice.
(G) *Aqp5* mRNA expression in the submandibular glands of NOD/ShiLtj mice injected with PBS, ADSC from WT or *Il33*$^{-/-}$ mice.
(H) Histology of the submandibular glands of NOD/ShiLtj mice injected with PBS, ADSC from WT or *Il33*$^{-/-}$ mice.
(I) The infiltrating area in the submandibular glands of NOD/ShiLtj mice injected with PBS, ADSC from WT or *Il33*$^{-/-}$ mice. Data are pooled from three independent experiments. One-way ANOVA was used. Scale bars, 100 μm and 50 μm; bars, mean; error bars, SEM. *$p < 0.05$, **$p < 0.01$, ***$p < 0.001$.

the decrease of IL-17 was independent of IL-33 (Figures S5B and S7B). In contrast to the submandibular glands, there was no significant difference in the frequency and number of CD4$^+$Foxp3$^+$ Tregs, ST2$^+$Tregs and Ki67$^+$ Tregs in the spleen, and armpit, inguinal and submandibular lymph nodes of all groups of NOD/ShiLtj mice (Figure S9). Taken together, these data indicate that mADSCs-IL-33-mediated suppression of inflammation and improvement of submandibular gland function was mainly ascribed to the enhanced number of ST2$^+$ Tregs and reduced the number of CD45$^+$ proinflammatory cells especially IFN-γ$^+$ T cells in the glands.

IL-1β upregulates IL-33 in human ADSCs

We next investigated whether human ADSCs also expressed IL-33 and IL-1β upregulated its expression. For this, we cultured human ADSCs with or without 2 ng/mL IL-1β for 6 and 24 h and then checked *IL33* mRNA and IL-33 protein, respectively. Untreated human ADSCs hardly exhibited IL-33; however, IL-1β treatment significantly upregulated the amount of *IL33* mRNA in human ADSCs at 6 h (Figure 6A). IL-33 protein was also increased significantly by IL-1β treatment in human ADSCs at 24 h (Figure 6B). We also studied the signal pathways for IL-33 production by human ADSCs in response to IL-1β. Consistent with murine ADSCs, the levels of phosphorylated ERK and p38 proteins were significantly increased in human ADSCs after IL-1β stimulation compared with the unstimulated cells (Figure 6C). Moreover, the selective protein kinase inhibitors (5Z)-7-oxozeaenol, U0126, and SB203580, which inhibit TAK1, ERK, and p38 MAPK, respectively, significantly decreased the inductive effect of IL-1β on *IL33* mRNA and IL-33 protein in human ADSCs (Figures 6D and 6E). TAK1 inhibitor also decreased the relative ratio of phosphorylated ERK/ERK and phosphorylated p38/p38 (Figure 6F). These data indicated that human ADSCs also produce IL-33 by IL-1β stimulation through TAK1-ERK/p38 signal pathways, suggesting a translational relevance and significance of the murine ADSCs treatment in animal SS models.

DISCUSSION

In this article, we demonstrated that ADSCs represent an important cellular source of IL-33 that could be induced specifically by IL-1β among the dozens of immune cytokines tested. We further elucidated that IL-1β-induced IL-33 production by ADSCs was mediated by TAK1-ERK/p38 signaling pathways. By using *Il33*$^{-/-}$ mice, we have uncovered that allogeneic ADSCs transplantation was able to suppress the inflammation and improve the saliva secretory function of salivary glands in NOD mice via an IL-33-dependent manner. Importantly, we have elucidated that the immunoregulatory function in SS by ADSCs-derived IL-33 is mediated mainly through upregulation of ST2$^+$ Tregs in the submandibular glands. Strikingly, we have shown that human ADSCs also produce IL-33 in response to IL-1β stimulation *in vitro*, suggesting a clinical relevance and significance in human diseases such as SS.

Several conclusions can be drawn from our findings. First, ADSCs are an important cellular source of IL-33 and IL-1β is the most important cytokine to induce IL-33 in ADSCs. IL-33 has been recognized as a unique but crucial regulatory cytokine in immunoregulation (Baumann et al., 2015; Gao et al., 2015; Hepworth et al., 2012; Price et al., 2010; Reichenbach et al., 2015; Yang et al., 2011) in several physiological and pathological settings such as autoimmunity, obesity, and allergy/asthma (Nakanishi et al., 2013; Nechama et al., 2018; Scott et al., 2018; Zhu et al., 2017). Several types of cells have been reported to produce IL-33 including endothelial cells (Chen et al., 2015), epithelial cells (Nakanishi et al., 2013), macrophages, dendritic cells, mast cells, and fibroblast-like cells (Moussion et al., 2008; Pichery et al., 2012) (Su et al., 2013; Xu et al., 2008) in response to certain stimuli such as LPS, IFN-γ, TNF-α, IL-3, IL-4, IL-17, and IL-1β (Meephansan et al., 2012, 2013; Su et al., 2013; Xu et al., 2008; Zhao and Hu, 2012). However, it was unknown whether MSCs could produce IL-33 until recently. Few studies have started to show that MSCs can produce IL-33 (Mahlakoiv et al., 2019), but what is the factor(s)/cytokines to stimulate MSCs to produce IL-33 remained unknown. We have here extended the studies by unambiguously proving that ADSCs indeed produce IL-33. Importantly, we have discovered that IL-1β is the critical factor in driving IL-33 expression in

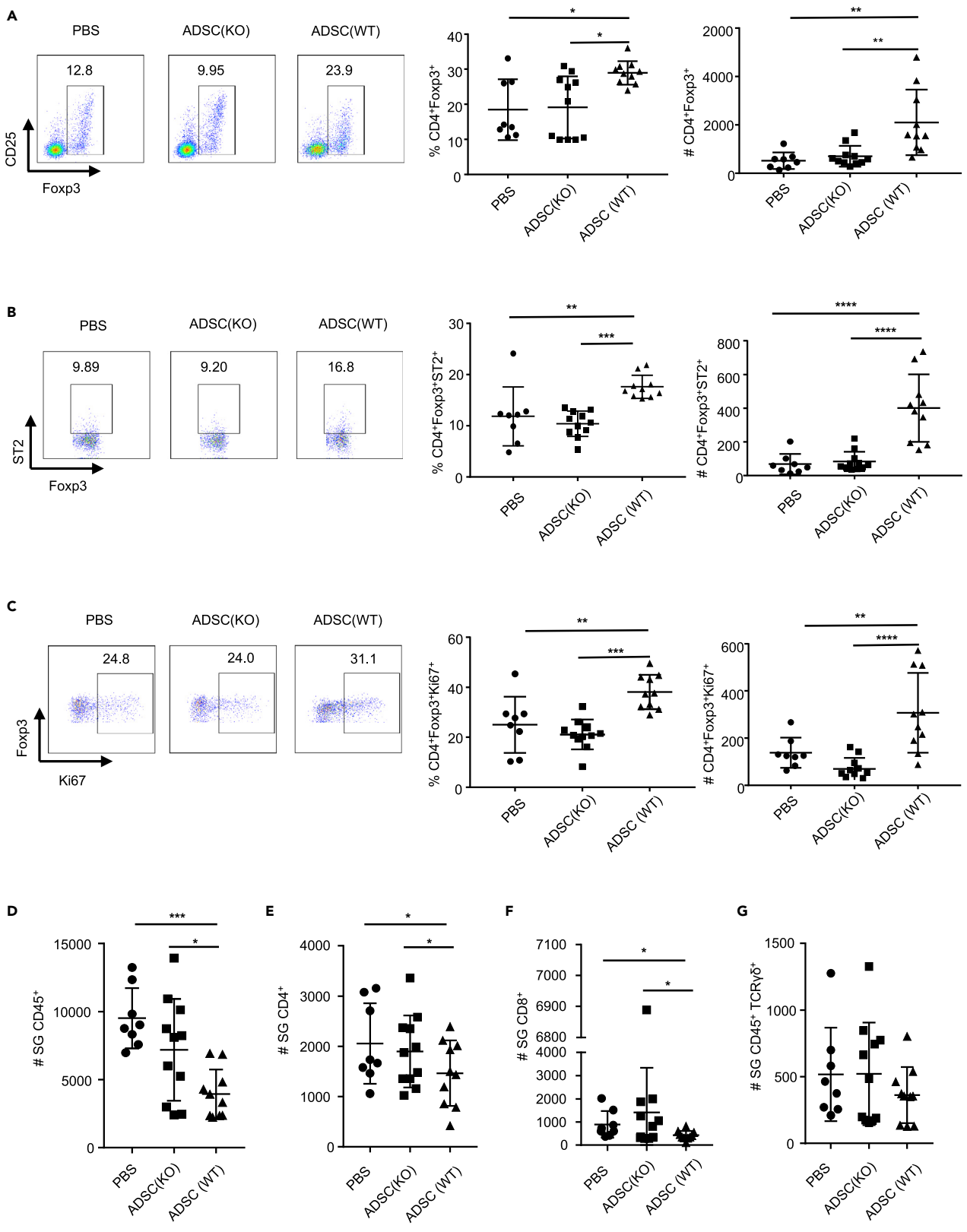
A
PBS
ADSC(KO)
ADSC(WT)
12.8
9.95
23.9
CD25
Foxp3
% CD4+Foxp3+
# CD4+Foxp3+
B
PBS
ADSC(KO)
ADSC(WT)
9.89
9.20
16.8
ST2
Foxp3
% CD4+Foxp3+ST2+
# CD4+Foxp3+ST2+
C
PBS
ADSC(KO)
ADSC(WT)
24.8
24.0
31.1
Foxp3
Ki67
% CD4+Foxp3+Ki67+
# CD4+Foxp3+Ki67+
D
SG CD45+
E
SG CD4+
F
SG CD8+
G
SG CD45+ TCRγδ+
PBS
ADSC(KO)
ADSC (WT)

Figure 5. WT ADSCs increase the frequency and an absolute number of CD4$^+$Foxp3$^+$ST2$^+$ Tregs in the submandibular glands of NOD/ShiLtj mice

(A) Frequency and absolute number of Foxp3$^+$ T cells in the submandibular glands of NOD/ShiLtj mice injected with PBS, ADSC from WT or *Il33*$^{-/-}$ mice.

(B) Frequency and absolute number of ST2$^+$ T cells in CD4$^+$Foxp3$^+$ T cell in the submandibular glands of NOD/ShiLtj mice injected with PBS, ADSC from WT or *Il33*$^{-/-}$ mice.

(C) Frequency and absolute number of Ki67$^+$ in CD4$^+$Foxp3$^+$ T cells in the submandibular glands of NOD/ShiLtj mice injected with PBS, ADSC from WT or *Il33*$^{-/-}$ mice.

(D) Absolute number of CD45$^+$ cells in the submandibular glands of NOD/ShiLtj mice injected with PBS, ADSC from WT or *Il33*$^{-/-}$ mice.

(E) Absolute number of CD45$^+$TCRβ$^+$CD4$^+$ cells per mg of submandibular gland of NOD/ShiLtj mice injected with PBS, ADSC from WT or *Il33*$^{-/-}$ mice.

(F) Absolute number of CD45$^+$TCRβ$^+$CD8$^+$ cells in the submandibular glands of NOD/ShiLtj mice injected with PBS, ADSC from WT or *Il33*$^{-/-}$ mice.

(G) Absolute number of CD45$^+$TCRγδ$^+$ cells in the submandibular glands of NOD/ShiLtj mice injected with PBS, ADSC from WT or *Il33*$^{-/-}$ mice. Data are pooled from three independent experiments. One-way ANOVA was used. Bars, mean; error bars, SEM; *p < 0.05, **p < 0.01, ***p < 0.001, ****p < 0.0001.

ADSCs. This finding is significant as it provides a previously unrecognized mechanism underlying MSCs-mediated immunoregulatory activities in the inflammatory tissues and organs and the paradoxical requirement of proinflammatory cytokines such as IL-1β (Bassi et al., 2012; Ding et al., 2010; Liu et al., 2013; Meisel et al., 2004). The specific stimulatory function for IL-1β in MSC-IL-33 production is unexpected but exciting. Although it is presently unknown why IL-1β, but not other proinflammatory cytokines such as TNF-α and IL-6, is the key to induce IL-33 secretion by ADSCs, it does suggest a possible functional link between IL-1β-producing cells and ADSCs. As IL-1β can be a cell membrane-bound form, this finding also suggests an interaction and functional regulation via a cell-cell contact manner, a fascinating question to be explored. The specific role of IL-1β in inducing IL-33 by ADSCs is further supported by the downstream molecular pathways that are involved in the effect, which is mainly mediated by ERK and p38 and TAK1, rather than NF-κB and JNK. As shown by qPCR analysis in Figures 1 and 5, we observed that human ADSCs expressed higher levels of IL-33 than did mouse ADSCs in response to their respective IL-1β stimulation. Although mechanistically still elusive, the species difference was reported before. For example, a study reported that human IL-33 was converted into more stable mature forms; however, mouse IL-33 was rapidly degraded (Cayrol et al., 2018). Thus further work is needed to understand the specific variation in the future.

Second, ADSCs can regulate inflammation and suppress autoimmunity in distant tissues and organs by producing IL-33. Supporting this conclusion includes that administration by intravenous injection of ADSCs from WT mice, but not from *Il33*$^{-/-}$ mice, effectively suppressed the ongoing inflammation in the submandibular glands and protected the secretary function of saliva in NOD mice. Our findings here provided a mechanism for the immunoregulatory effect of allogenic ADSCs through an IL-33-dependent mechanism.

Moreover, we found that the immunoregulatory function of ADSC-derived IL-33 is mainly through the expansion of ST2$^+$ Tregs in the submandibular glands. Several pieces of evidence support this conclusion: *in vitro*, WT, but not *Il33*$^{-/-}$, ADSCs-mediated expansion of Tregs are primarily restricted to the ST2$^+$ Tregs. In contrast, ADSCs fail to convert naive CD4$^+$ T cells to Foxp3$^+$ Tregs, consistent with the notion that TGF-β (Chen et al., 2003) rather than IL-33 is the primary driving force to induce Foxp3 from naive CD4$^+$ T cells. IL-33 is the cytokine to expand ST2$^+$ Tregs. This IL-33-driven ST2$^+$ Treg expansion was confirmed in the submandibular glands in SS NOD mice. Administration of WT, but not *Il33*$^{-/-}$, ADSCs significantly expand ST2$^+$ Tregs in the submandibular glands of SS mice, which consequently protects the function of salivary glands. Notably, the increase in ST2$^+$ Tregs in the submandibular glands is not only restricted to the frequency but also the absolute number of the ST2$^+$ Tregs, further confirming the real growth of the Tregs by IL-33. The significant expansion of ST2$^+$ Tregs in the submandibular glands plays an important role in suppressing the inflammation of the tissue. This is supported by the significant decrease in the absolute number of infiltrated CD45$^+$ proinflammatory cells in the submandibular glands of SS-like NOD mice treated with WT ADSCs. IL-13-producing T cells have been implicated in the pathogenesis of an SS animal model that is induced by the deficiency of transcriptional factor Id3 (Li et al., 2004). However, we did not find that IL-13$^+$ T cells were changed by ADSCs treatment, suggesting the ADSCs-IL-33 functioning NOD model was not primarily by affecting IL-13$^+$ Th2 cells. Of note, WT ADSCs treatment surprisingly increased the frequency and number of CD8$^+$IL-4$^+$ T cells in the submandibular glands; although the overall frequency is low, it remains to be known whether these IL-4$^+$ T cells play any function in the immunoregulatory effects on SS. The suppressive function of Tregs and ST2$^+$ Tregs in immune cells and responses has been validated in many *in vitro* and *in vivo* settings in the literature, including in NOD mice (Alunno et al., 2015; Burzyn et al., 2013; Katsifis et al., 2007; Sarigul et al., 2010).

Third, IL-33 can be produced by ADSC with IL-1β stimulation, although IL-33 but cannot be secreted. Supporting this conclusion includes that IL-33 was hardly detected in the cell culture supernatants, although

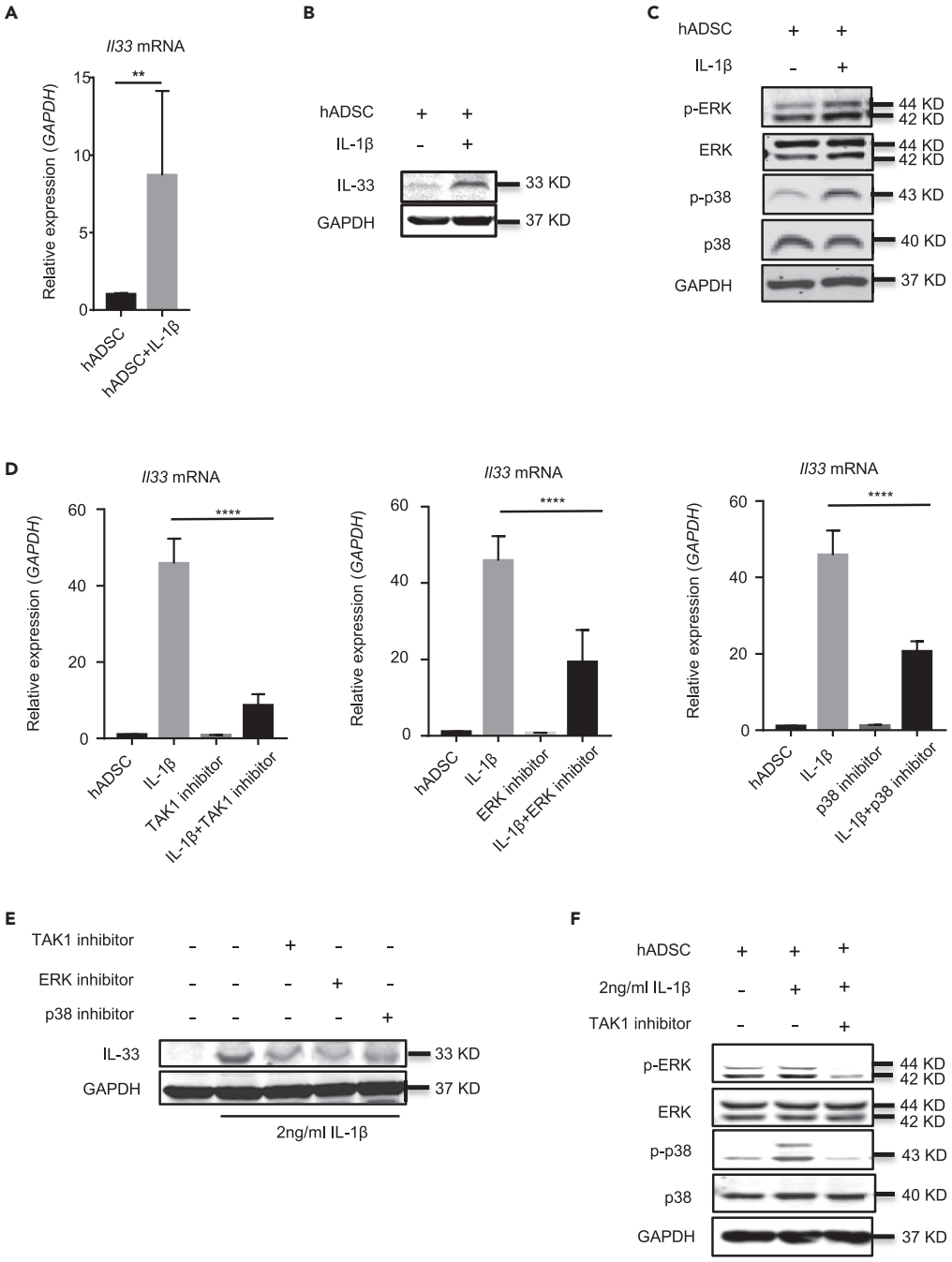

Figure 6. IL-1β upregulates IL-33 expression in human ADSCs

(A) *Il33* mRNA expression in human ADSC stimulated for 6 h with or without 2 ng/mL IL-1β.

(B) Western blot of IL-33 and GAPDH in human ADSC stimulated with or without 2 ng/mL IL-1β for 24 h.

(C) Western blot of p-ERK, ERK, p-p38, p38, and GAPDH in human ADSC stimulated with or without IL-1β for 2 h

(D) *Il33* mRNA expression in human ADSC stimulated for 6 h with or without IL-1β, TAK1 inhibitor, ERK inhibitor, or p38 inhibitor for 6 h.

(E) Western blot of IL-33 and GAPDH in human ADSC stimulated with or without IL-1β, TAK1 inhibitor, ERK inhibitor, or p38 inhibitor for 24 h.

(F) Western blot of p-ERK, ERK, p-p38, p38, and GAPDH in human ADSC stimulated with or without IL-1β, TAK1 inhibitor for 1 h. Data are pooled from three (A and D) independent experiments or are representative of three (B, C, E and F) independent experiments. In (A), Student's t test was used. In (D), one-way ANOVA was used. Bars, mean; error bars, SEM; $^{**}p < 0.01$, $^{****}p < 0.0001$.

ELISA analysis also showed higher levels of IL-33 protein in the cell lysates from IL-1β-treated ADSCs compared with the untreated cells. Moreover, the cell lysates from IL-1β-stimulated WT ADSCs significantly upregulated *Il1rl1* mRNA (receptor for IL-33, ST2) expression in Tregs. There must be a way for MSCs *in vivo* to be equipped functionally and recruited accurately to damaged tissue. Several researches have proved that following intravenous infusion of MSC populations expanded *in vitro*, almost 80% MSCs are trapped in the lungs, and these cells in lung disappeared with a half-life of about 24 h; some MSCs subsequently become home to damaged tissue (Barbash et al., 2003; Lee et al., 2009). We have also previously reported that allogenic MSCs could exhibit protective effects on SS development in mice by showing that MSCs could migrate into the submandibular glands to function (Xu et al., 2012). Therefore, the therapeutic effects of MSCs may depend mainly on the release of IL-33 of dead MSCs to regulate inflammation and tissue homeostasis.

Finally, the ADSCs-IL-33 may also play an important role in MSC-mediated immunoregulation in relevant human autoimmune diseases like SS. Supporting this conclusion include our findings that human ADSCs also produce IL-33, which is also triggered by IL-1β stimulation *in vitro*. Although it still needs to be confirmed in the patients, our experimental evidence indeed shows the clinical relevance of our animal studies.

In sum, we have discovered that adipose tissues contain MSCs that produce IL-33 in response to proinflammatory cytokine IL-1β. This MSC-derived IL-33 can suppress inflammation in organ-specific autoimmunity such as SS through specifically expanding $ST2^{+}$ Tregs. Our findings may be clinically and translationally relevant, as human ADSCs also produce IL-33 in response to IL-1β. These findings collectively should have implications for better manipulation of allogeneic MSCs in relevant human autoimmune diseases such as SS.

Limitations of the study

There are still some limitations in our study. For example, it remains to be elucidated how important IL-1β-mediated increase in IL-33 from ADSC is in the SS model. The technical challenge and difficulty prevented us to use ST2 knockout Tregs to provide further evidence of IL-33/ST2 pathway in Treg-mediated suppression of SS models, which we will address in the future. Moreover, it would be interesting to investigate whether ADSC-derived IL-33 has any effects on Treg function through their ST2 receptors in patients with SS.

Resource availability

Lead contact

Further information and requests for resources and reagents should be directed to and will be fulfilled by the lead contact, Wanjun Chen(wchen@dir.nidcr.nih.gov).

Materials availability

This study did not generate new unique reagents.

Data and code accessibility

This study did not generate/analyze datasets and code.

METHODS

All methods can be found in the accompanying Transparent methods supplemental file.

SUPPLEMENTAL INFORMATION

Supplemental information can be found online at https://doi.org/10.1016/j.isci.2021.102446.

ACKNOWLEDGMENTS

We thank Dr. M. Colonna, Dept of Pathology and Immunology, Washington University, MO, USA, for *C57BL/6J-Il33*$^{tm1b(EUCOMM)Cln}$. We also thank the NIDCR CTRC and VRC for their technical support. This work was supported by the Intramural Research Program of the National Institute of Dental and

Craniofacial Research (US National Institutes of Health). This work was also supported by the grant from the National Natural Science Foundation of China (81970905 to O.S.L.).

AUTHOR CONTRIBUTIONS

O.L. and J.X. designed and performed experiments, analyzed and interpreted the data, and drafted the manuscript; F.W., W.J., N.G., P.Z., N.G., Y.H., and A.B. performed experiments; G.M., S.W., and Z. T. provided critical input and/or support. W.C. conceived and supervised the whole study, designed the experiments, and wrote the manuscript.

DECLARATION OF INTERESTS

The authors declare no competing interests.

Received: December 23, 2020
Revised: March 11, 2021
Accepted: April 14, 2021
Published: May 21, 2021

REFERENCES

Alexeev, V., Arita, M., Donahue, A., Bonaldo, P., Chu, M.L., and Igoucheva, O. (2014). Human adipose-derived stem cell transplantation as a potential therapy for collagen VI-related congenital muscular dystrophy. Stem Cell Res. Ther. *5*, 21.

Ali, S., Mohs, A., Thomas, M., Klare, J., Ross, R., Schmitz, M.L., and Martin, M.U. (2011). The dual function cytokine IL-33 interacts with the transcription factor NF-kappaB to dampen NF-kappaB-stimulated gene transcription. J. Immunol. *187*, 1609–1616.

Alunno, A., Carubbi, F., Bistoni, O., Caterbi, S., Bartoloni, E., Mirabelli, G., Cannarile, F., Cipriani, P., Giacomelli, R., and Gerli, R. (2015). T regulatory and T helper 17 cells in primary Sjogren's syndrome: facts and perspectives. Mediators Inflamm. *2015*, 243723.

Arpaia, N., Green, J.A., Moltedo, B., Arvey, A., Hemmers, S., Yuan, S., Treuting, P.M., and Rudensky, A.Y. (2015). A distinct function of regulatory T cells in tissue protection. Cell *162*, 1078–1089.

Barbash, I.M., Chouraqui, P., Baron, J., Feinberg, M.S., Etzion, S., Tessone, A., Miller, L., Guetta, E., Zipori, D., Kedes, L.H., et al. (2003). Systemic delivery of bone marrow-derived mesenchymal stem cells to the infarcted myocardium: feasibility, cell migration, and body distribution. Circulation *108*, 863–868.

Bassi, E.J., Moraes-Vieira, P.M., Moreira-Sa, C.S., Almeida, D.C., Vieira, L.M., Cunha, C.S., Hiyane, M.I., Basso, A.S., Pacheco-Silva, A., and Camara, N.O. (2012). Immune regulatory properties of allogeneic adipose-derived mesenchymal stem cells in the treatment of experimental autoimmune diabetes. Diabetes *61*, 2534–2545.

Baumann, C., Bonilla, W.V., Frohlich, A., Helmstetter, C., Peine, M., Hegazy, A.N., Pinschewer, D.D., and Lohning, M. (2015). T-bet- and STAT4-dependent IL-33 receptor expression directly promotes antiviral Th1 cell responses. Proc. Natl. Acad. Sci. U S A *112*, 4056–4061.

Bourin, P., Bunnell, B.A., Casteilla, L., Dominici, M., Katz, A.J., March, K.L., Redl, H., Rubin, J.P., Yoshimura, K., and Gimble, J.M. (2013). Stromal cells from the adipose tissue-derived stromal vascular fraction and culture expanded adipose tissue-derived stromal/stem cells: a joint statement of the International Federation for Adipose Therapeutics and Science (IFATS) and the International Society for Cellular Therapy (ISCT). Cytotherapy *15*, 641–648.

Burzyn, D., Kuswanto, W., Kolodin, D., Shadrach, J.L., Cerletti, M., Jang, Y., Sefik, E., Tan, T.G., Wagers, A.J., Benoist, C., et al. (2013). A special population of regulatory T cells potentiates muscle repair. Cell *155*, 1282–1295.

Castelo-Branco, M.T., Soares, I.D., Lopes, D.V., Buongusto, F., Martinusso, C.A., do Rosario, A., Jr., Souza, S.A., Gutfilen, B., Fonseca, L.M., Elia, C., et al. (2012). Intraperitoneal but not intravenous cryopreserved mesenchymal stromal cells home to the inflamed colon and ameliorate experimental colitis. PLoS One *7*, e33360.

Cayrol, C., Duval, A., Schmitt, P., Roga, S., Camus, M., Stella, A., Burlet-Schiltz, O., Gonzalez-de-Peredo, A., and Girard, J. (2018). Environmental allergens induce allergic inflammation through proteolytic maturation of IL-33. Nat. Immunol. *19*, 375–385.

Chen, Q.Q., Yan, L., Wang, C.Z., Wang, W.H., Shi, H., Su, B.B., Zeng, Q.H., Du, H.T., and Wan, J. (2013). Mesenchymal stem cells alleviate TNBS-induced colitis by modulating inflammatory and autoimmune responses. World J. Gastroenterol. *19*, 4702–4717.

Chen, W., Jin, W., Hardegen, N., Lei, K.J., Li, L., Marinos, N., McGrady, G., and Wahl, S.M. (2003). Conversion of peripheral CD4+CD25- naive T cells to CD4+CD25+ regulatory T cells by TGF-beta induction of transcription factor Foxp3. J. Exp. Med. *198*, 1875–1886.

Chen, W.Y., Hong, J., Gannon, J., Kakkar, R., and Lee, R.T. (2015). Myocardial pressure overload induces systemic inflammation through endothelial cell IL-33. Proc. Natl. Acad. Sci. U S A *112*, 7249–7254.

Delaleu, N., Nguyen, C.Q., Peck, A.B., and Jonsson, R. (2011). Sjogren's syndrome: studying the disease in mice. Arthritis Res. Ther. *13*, 217.

Ding, G., Liu, Y., Wang, W., Wei, F., Liu, D., Fan, Z., An, Y., Zhang, C., and Wang, S. (2010). Allogeneic periodontal ligament stem cell therapy for periodontitis in swine. Stem Cells *28*, 1829–1838.

Gao, X., Wang, X., Yang, Q., Zhao, X., Wen, W., Li, G., Lu, J., Qin, W., Qi, Y., Xie, F., et al. (2015). Tumoral expression of IL-33 inhibits tumor growth and modifies the tumor microenvironment through CD8+ T and NK cells. J. Immunol. *194*, 438–445.

Gonzalez, M.A., Gonzalez-Rey, E., Rico, L., Buscher, D., and Delgado, M. (2009a). Adipose-derived mesenchymal stem cells alleviate experimental colitis by inhibiting inflammatory and autoimmune responses. Gastroenterology *136*, 978–989.

Gonzalez, M.A., Gonzalez-Rey, E., Rico, L., Buscher, D., and Delgado, M. (2009b). Treatment of experimental arthritis by inducing immune tolerance with human adipose-derived mesenchymal stem cells. Arthritis Rheum. *60*, 1006–1019.

Hepworth, M.R., Maurer, M., and Hartmann, S. (2012). Regulation of type 2 immunity to helminths by mast cells. Gut Microbes *3*, 476–481.

Katsifis, G.E., Moutsopoulos, N.M., and Wahl, S.M. (2007). T lymphocytes in Sjogren's syndrome: contributors to and regulators of pathophysiology. Clin. Rev. Allergy Immunol. *32*, 252–264.

Krampera, M., Cosmi, L., Angeli, R., Pasini, A., Liotta, F., Andreini, A., Santarlasci, V., Mazzinghi, B., Pizzolo, G., Vinante, F., et al. (2006). Role for interferon-gamma in the immunomodulatory activity of human bone marrow mesenchymal stem cells. Stem Cells *24*, 386–398.

Lee, R.H., Pulin, A.A., Seo, M.J., Kota, D.J., Ylostalo, J., Larson, B.L., Semprun-Prieto, L., Delafontaine, P., and Prockop, D.J. (2009). Intravenous hMSCs improve myocardial

infarction in mice because cells embolized in lung are activated to secrete the anti-inflammatory protein TSG-6. Cell Stem Cell *5*, 54–63.

Li, H., Dai, M., and Zhuang, Y. (2004). A T cell intrinsic role of Id3 in a mouse model for primary Sjogren's syndrome. Immunity *21*, 551–560.

Licona-Limon, P., Kim, L.K., Palm, N.W., and Flavell, R.A. (2013). TH2, allergy and group 2 innate lymphoid cells. Nat. Immunol. *14*, 536–542.

Liew, F.Y., Girard, J.P., and Turnquist, H.R. (2016). Interleukin-33 in health and disease. Nat. Rev. Immunol. *16*, 676–689.

Liu, O., Xu, J., Ding, G., Liu, D., Fan, Z., Zhang, C., Chen, W., Ding, Y., Tang, Z., and Wang, S. (2013). Periodontal ligament stem cells regulate B lymphocyte function via programmed cell death protein 1. Stem Cells *31*, 1371–1382.

Mahlakoiv, T., Flamar, A.L., Johnston, L.K., Moriyama, S., Putzel, G.G., Bryce, P.J., and Artis, D. (2019). Stromal cells maintain immune cell homeostasis in adipose tissue via production of interleukin-33. Sci. Immunol. *4*, eaax0416.

Markadieu, N., and Delpire, E. (2014). Physiology and pathophysiology of SLC12A1/2 transporters. Pflugers Arch. *466*, 91–105.

Matta, B.M., Reichenbach, D.K., Zhang, X., Mathews, L., Koehn, B.H., Dwyer, G.K., Lott, J.M., Uhl, F.M., Pfeifer, D., Feser, C.J., et al. (2016). Peri-alloHCT IL-33 administration expands recipient T-regulatory cells that protect mice against acute GVHD. Blood *128*, 427–439.

Meephansan, J., Komine, M., Tsuda, H., Karakawa, M., Tominaga, S., and Ohtsuki, M. (2013). Expression of IL-33 in the epidermis: the mechanism of induction by IL-17. J. Dermatol. Sci. *71*, 107–114.

Meephansan, J., Tsuda, H., Komine, M., Tominaga, S., and Ohtsuki, M. (2012). Regulation of IL-33 expression by IFN-gamma and tumor necrosis factor-alpha in normal human epidermal keratinocytes. J. Invest. Dermatol. *132*, 2593–2600.

Meisel, R., Zibert, A., Laryea, M., Gobel, U., Daubener, W., and Dilloo, D. (2004). Human bone marrow stromal cells inhibit allogeneic T-cell responses by indoleamine 2,3-dioxygenase-mediated tryptophan degradation. Blood *103*, 4619–4621.

Mizuno, H., Tobita, M., and Uysal, A.C. (2012). Concise review: adipose-derived stem cells as a novel tool for future regenerative medicine. Stem Cells *30*, 804–810.

Molofsky, A.B., Nussbaum, J.C., Liang, H.E., Van Dyken, S.J., Cheng, L.E., Mohapatra, A., Chawla, A., and Locksley, R.M. (2013). Innate lymphoid type 2 cells sustain visceral adipose tissue eosinophils and alternatively activated macrophages. J. Exp. Med. *210*, 535–549.

Molofsky, A.B., Savage, A.K., and Locksley, R.M. (2015a). Interleukin-33 in tissue homeostasis, injury, and inflammation. Immunity *42*, 1005–1019.

Molofsky, A.B., Van Gool, F., Liang, H.E., Van Dyken, S.J., Nussbaum, J.C., Lee, J., Bluestone, J.A., and Locksley, R.M. (2015b). Interleukin-33 and interferon-gamma counter-regulate group 2 innate lymphoid cell activation during immune perturbation. Immunity *43*, 161–174.

Moro, K., Yamada, T., Tanabe, M., Takeuchi, T., Ikawa, T., Kawamoto, H., Furusawa, J., Ohtani, M., Fujii, H., and Koyasu, S. (2010). Innate production of T(H)2 cytokines by adipose tissue-associated c-Kit(+)Sca-1(+) lymphoid cells. Nature *463*, 540–544.

Mougiakakos, D., Jitschin, R., Johansson, C.C., Okita, R., Kiessling, R., and Le Blanc, K. (2011). The impact of inflammatory licensing on heme oxygenase-1-mediated induction of regulatory T cells by human mesenchymal stem cells. Blood *117*, 4826–4835.

Moussion, C., Ortega, N., and Girard, J.P. (2008). The IL-1-like cytokine IL-33 is constitutively expressed in the nucleus of endothelial cells and epithelial cells in vivo: a novel 'alarmin'? PLoS One *3*, e3331.

Nakanishi, W., Yamaguchi, S., Matsuda, A., Suzukawa, M., Shibui, A., Nambu, A., Kondo, K., Suto, H., Saito, H., Matsumoto, K., et al. (2013). IL-33, but not IL-25, is crucial for the development of house dust mite antigen-induced allergic rhinitis. PLoS One *8*, e78099.

Nechama, M., Kwon, J., Wei, S., Kyi, A.T., Welner, R.S., Ben-Dov, I.Z., Arredouani, M.S., Asara, J.M., Chen, C.H., Tsai, C.Y., et al. (2018). The IL-33-PIN1-IRAK-M axis is critical for type 2 immunity in IL-33-induced allergic airway inflammation. Nat. Commun. *9*, 1603.

Pichery, M., Mirey, E., Mercier, P., Lefrancais, E., Dujardin, A., Ortega, N., and Girard, J.P. (2012). Endogenous IL-33 is highly expressed in mouse epithelial barrier tissues, lymphoid organs, brain, embryos, and inflamed tissues: in situ analysis using a novel Il-33-LacZ gene trap reporter strain. J. Immunol. *188*, 3488–3495.

Price, A.E., Liang, H.E., Sullivan, B.M., Reinhardt, R.L., Eisley, C.J., Erle, D.J., and Locksley, R.M. (2010). Systemically dispersed innate IL-13-expressing cells in type 2 immunity. Proc. Natl. Acad. Sci. U S A *107*, 11489–11494.

Razmkhah, M., Abedi, N., Hosseini, A., Imani, M.T., Talei, A.R., and Ghaderi, A. (2015). Induction of T regulatory subsets from naive CD4+ T cells after exposure to breast cancer adipose derived stem cells. Iran. J. Immunol. *12*, 1–15.

Reichenbach, D.K., Schwarze, V., Matta, B.M., Tkachev, V., Lieberknecht, E., Liu, Q., Koehn, B.H., Pfeifer, D., Taylor, P.A., Prinz, G., et al. (2015). The IL-33/ST2 axis augments effector T-cell responses during acute GVHD. Blood *125*, 3183–3192.

Ren, G., Su, J., Zhang, L., Zhao, X., Ling, W., L'Huillie, A., Zhang, J., Lu, Y., Roberts, A.I., Ji, W., et al. (2009). Species variation in the mechanisms of mesenchymal stem cell-mediated immunosuppression. Stem Cells *27*, 1954–1962.

Ren, G., Zhang, L., Zhao, X., Xu, G., Zhang, Y., Roberts, A.I., Zhao, R.C., and Shi, Y. (2008). Mesenchymal stem cell-mediated immunosuppression occurs via concerted action of chemokines and nitric oxide. Cell Stem Cell *2*, 141–150.

Sarigul, M., Yazisiz, V., Bassorgun, C.I., Ulker, M., Avci, A.B., Erbasan, F., Gelen, T., Gorczynski, R.M., and Terzioglu, E. (2010). The numbers of Foxp3 + Treg cells are positively correlated with higher grade of infiltration at the salivary glands in primary Sjogren's syndrome. Lupus *19*, 138–145.

Schiering, C., Krausgruber, T., Chomka, A., Frohlich, A., Adelmann, K., Wohlfert, E.A., Pott, J., Griseri, T., Bollrath, J., Hegazy, A.N., et al. (2014). The alarmin IL-33 promotes regulatory T-cell function in the intestine. Nature *513*, 564–568.

Schmitz, J., Owyang, A., Oldham, E., Song, Y., Murphy, E., McClanahan, T.K., Zurawski, G., Moshrefi, M., Qin, J., Li, X., et al. (2005). IL-33, an interleukin-1-like cytokine that signals via the IL-1 receptor-related protein ST2 and induces T helper type 2-associated cytokines. Immunity *23*, 479–490.

Scott, I.C., Majithiya, J.B., Sanden, C., Thornton, P., Sanders, P.N., Moore, T., Guscott, M., Corkill, D.J., Erjefalt, J.S., and Cohen, E.S. (2018). Interleukin-33 is activated by allergen- and necrosis-associated proteolytic activities to regulate its alarmin activity during epithelial damage. Sci. Rep. *8*, 3363.

Shang, Q., Bai, Y., Wang, G., Song, Q., Guo, C., Zhang, L., and Wang, Q. (2015). Delivery of adipose-derived stem cells attenuates adipose tissue inflammation and insulin resistance in obese mice through remodeling macrophage phenotypes. Stem Cells Dev. *24*, 2052–2064.

Sheng, H., Wang, Y., Jin, Y., Zhang, Q., Zhang, Y., Wang, L., Shen, B., Yin, S., Liu, W., Cui, L., et al. (2008). A critical role of IFNgamma in priming MSC-mediated suppression of T cell proliferation through up-regulation of B7-H1. Cell Res. *18*, 846–857.

Su, Z., Lin, J., Lu, F., Zhang, X., Zhang, L., Gandhi, N.B., de Paiva, C.S., Pflugfelder, S.C., and Li, D.Q. (2013). Potential autocrine regulation of interleukin-33/ST2 signaling of dendritic cells in allergic inflammation. Mucosal Immunol. *6*, 921–930.

Tanaka, F., Tominaga, K., Ochi, M., Tanigawa, T., Watanabe, T., Fujiwara, Y., Ohta, K., Oshitani, N., Higuchi, K., and Arakawa, T. (2008). Exogenous administration of mesenchymal stem cells ameliorates dextran sulfate sodium-induced colitis via anti-inflammatory action in damaged tissue in rats. Life Sci. *83*, 771–779.

Vasanthakumar, A., Moro, K., Xin, A., Liao, Y., Gloury, R., Kawamoto, S., Fagarasan, S., Mielke, L.A., Afshar-Sterle, S., Masters, S.L., et al. (2015). The transcriptional regulators IRF4, BATF and IL-33 orchestrate development and maintenance of adipose tissue-resident regulatory T cells. Nat. Immunol. *16*, 276–285.

Wang, S.Q., Wang, Y.X., and Hua, H. (2017). Characteristics of labial gland mesenchymal stem cells of healthy individuals and patients with Sjogren's syndrome: a preliminary study. Stem Cells Dev. *26*, 1171–1185.

Xu, D., Jiang, H.R., Kewin, P., Li, Y., Mu, R., Fraser, A.R., Pitman, N., Kurowska-Stolarska, M., McKenzie, A.N., McInnes, I.B., et al. (2008). IL-33 exacerbates antigen-induced arthritis by activating mast cells. Proc. Natl. Acad. Sci. U S A *105*, 10913–10918.

Xu, J., Wang, D., Liu, D., Fan, Z., Zhang, H., Liu, O., Ding, G., Gao, R., Zhang, C., Ding, Y., et al. (2012). Allogeneic mesenchymal stem cell treatment alleviates experimental and clinical Sjogren syndrome. Blood *120*, 3142–3151.

Yang, Q., Li, G., Zhu, Y., Liu, L., Chen, E., Turnquist, H., Zhang, X., Finn, O.J., Chen, X., and Lu, B. (2011). IL-33 synergizes with TCR and IL-12 signaling to promote the effector function of CD8+ T cells. Eur. J. Immunol. *41*, 3351–3360.

Zhao, W.H., and Hu, Z.Q. (2012). Up-regulation of IL-33 expression in various types of murine cells by IL-3 and IL-4. Cytokine *58*, 267–273.

Zhu, J., Xu, Y., Zhu, C., Zhao, J., Meng, X., Chen, S., Wang, T., Li, X., Zhang, L., Lu, C., et al. (2017). IL-33 induces both regulatory B cells and regulatory T cells in dextran sulfate sodium-induced colitis. Int. Immunopharmacol. *46*, 38–47.

Zuk, P., Zhu, M., Mizuno, H., Huang, J., Futrell, J., Katz, A., Benhaim, P., Lorenz, H., and Hedrick, M. (2001). Multilineage cells from human adipose tissue: implications for cell-based therapies. Tissue Eng. *7*, 211–228.

iScience, Volume *24*

Supplemental information

Adipose-mesenchymal stromal cells suppress experimental Sjögren syndrome by IL-33-driven expansion of ST2^{+} regulatory T cells

Ousheng Liu, Junji Xu, Fu Wang, Wenwen Jin, Peter Zanvit, Dandan Wang, Nathan Goldberg, Alexander Cain, Nancy Guo, Yichen Han, Andrew Bynum, Guowu Ma, Songlin Wang, Zhangui Tang, and Wanjun Chen

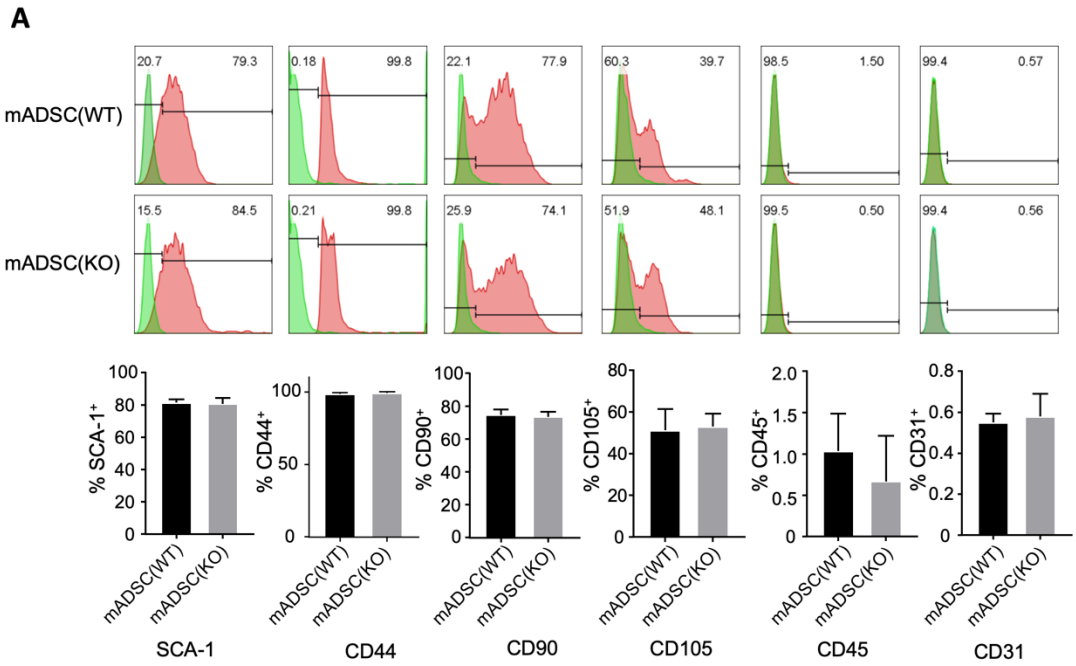
A
mADSC(WT)
mADSC(KO)
20.7
79.3
0.18
99.8
22.1
77.9
60.3
39.7
98.5
1.50
99.4
0.57
15.5
84.5
0.21
99.8
25.9
74.1
51.9
48.1
99.5
0.50
99.4
0.56
% SCA-1+
% CD44+
% CD90+
% CD105+
% CD45+
% CD31+
mADSC(WT)
mADSC(KO)
SCA-1
CD44
CD90
CD105
CD45
CD31

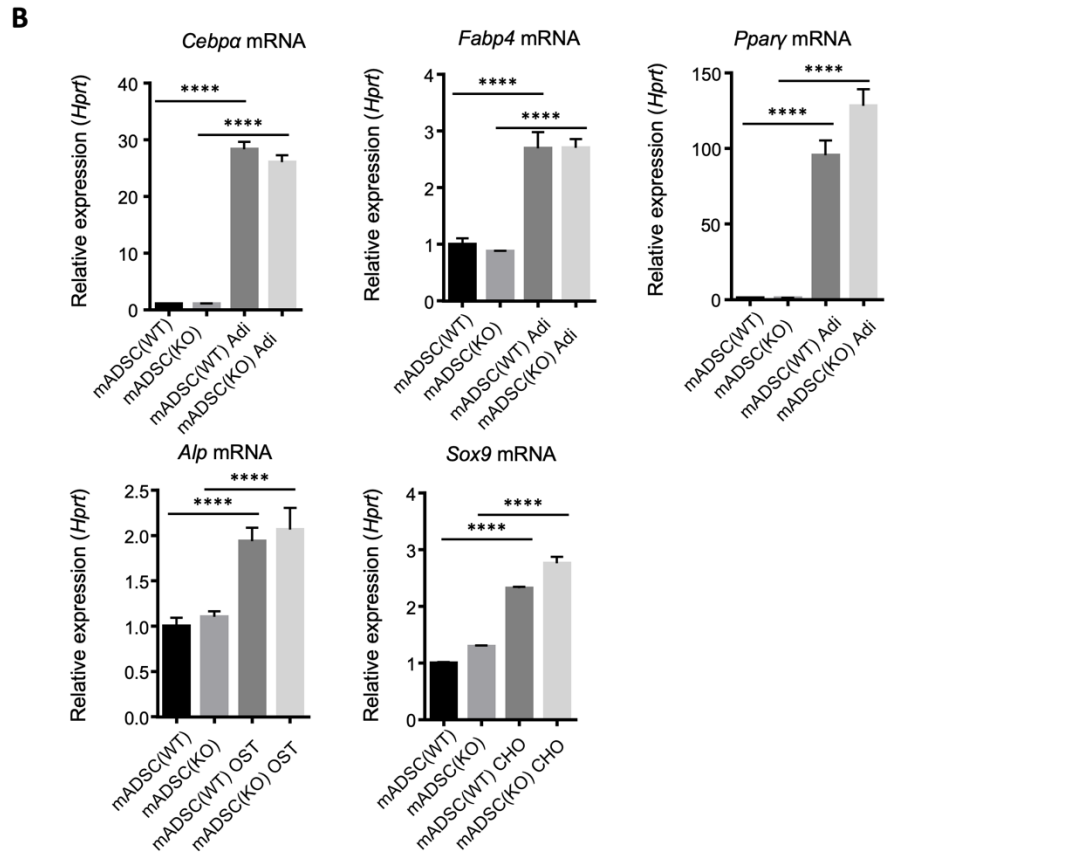
B
Cebpα mRNA
Fabp4 mRNA
Pparγ mRNA
Alp mRNA
Sox9 mRNA
Relative expression (Hprt)
****
mADSC(WT)
mADSC(KO)
mADSC(WT) Adi
mADSC(KO) Adi
mADSC(WT) OST
mADSC(KO) OST
mADSC(WT) CHO
mADSC(KO) CHO

Figure S1. Characterization of the immunophenotype and differentiation potential of mADSC from C57BL/6 or C57BL/6J-*Il33*$^{tm1b(EUCOMM)Cln}$ *in vitro*. Related to Figure 1.

(A) mADSCs from C57BL/6 or C57BL/6J-*Il33*$^{tm1b(EUCOMM)Cln}$ express MSC markers.

(B) mADSCs from C57BL/6 or C57BL/6J-*Il33*$^{tm1b(EUCOMM)Cln}$ were capable of differentiating into adipocytes, osteoblasts, and chondroblast under inductive culture conditions.

Data are pooled from three (A,B) independent experiments. One-way ANOVA was used. Bars, mean; error bars, SEM; ****$P < 0.0001$.

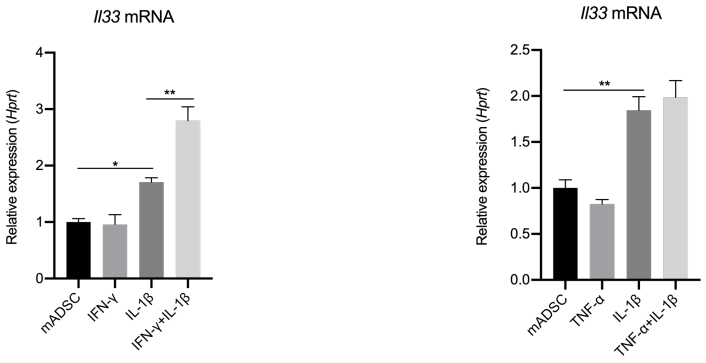

Figure S2. Expression pattern of IL-33 induced by IL-1β synergistically work with TNF-α and IFN-γ. Related Figure 2.

Il33 mRNA expression in mADSC stimulated with indicated combinations of recombinant cytokines (10 ng/ml each) for 6 hr.

Data are pooled from three independent experiments. One-way ANOVA was used. Bars, mean; error bars, SEM; **P*< 0.05, ***P* < 0.01.

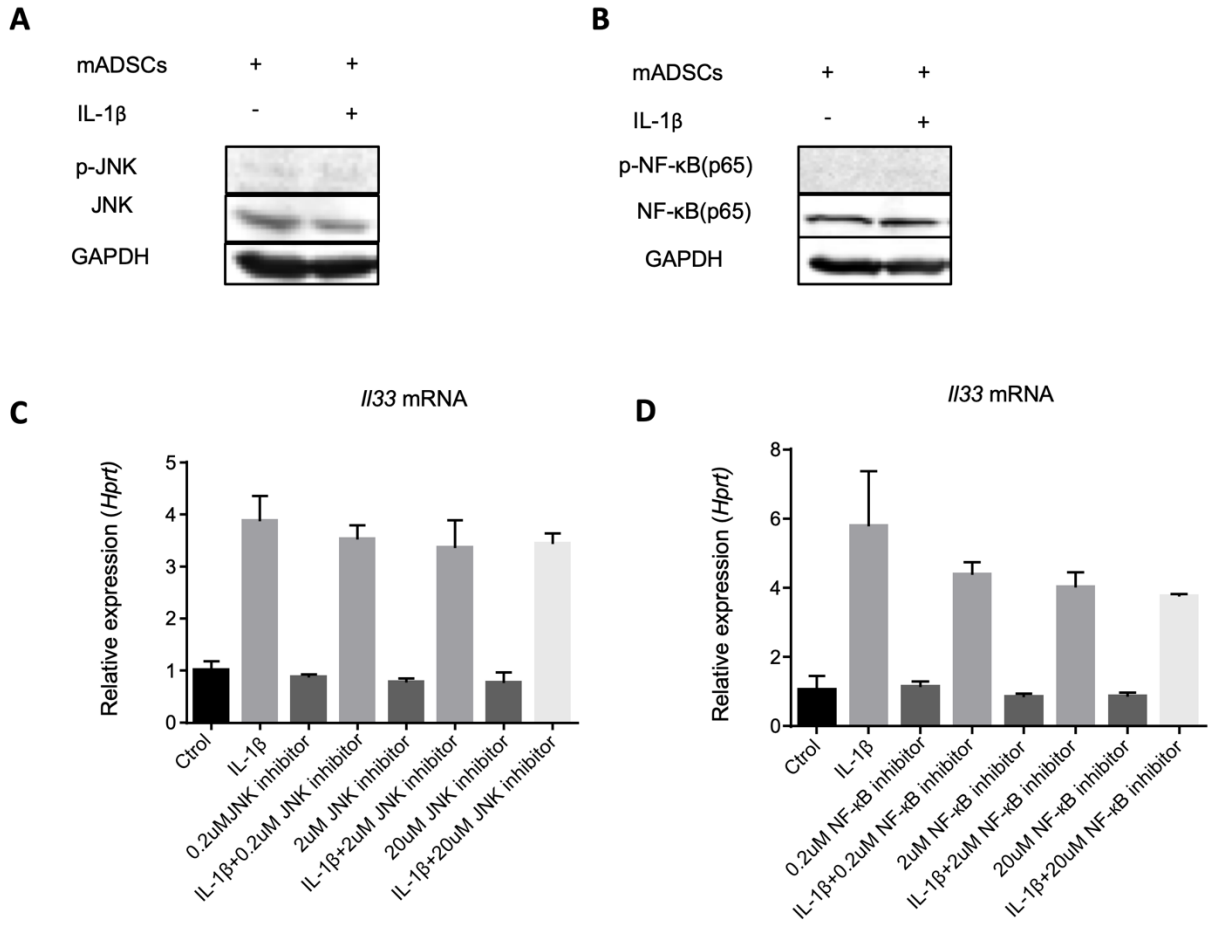

Figure S3. IL-1β upregulates IL-33 expression in mADSC independent on JNK and NF-κB(p65) pathways. Related to Figure 2.

(A) Western blot of p-JNK, JNK, and GAPDH in m ADSC stimulated with or without 2ng/ml IL-1β for 2 hr.

(B) Western blot of p-NF-kB(p65), NF-kB(p65) and GAPDH in m ADSC stimulated with or without IL-1β for 2 hr.

(C) *Il33* mRNA expression in mADSC stimulated for 6 hr with or without 2ng/ml IL-1β plus indicated the concentration of SP600125.

(D) *Il33* mRNA expression in mADSC stimulated for 6 hr with or without 2ng/ml IL-1β plus indicated the concentration of JSH23.

Data are pooled from three (C and D) independent experiments or are representative of three (A and B) independent experiments. In (C and D), one-way ANOVA was used. Bars, mean; error bars, SEM.

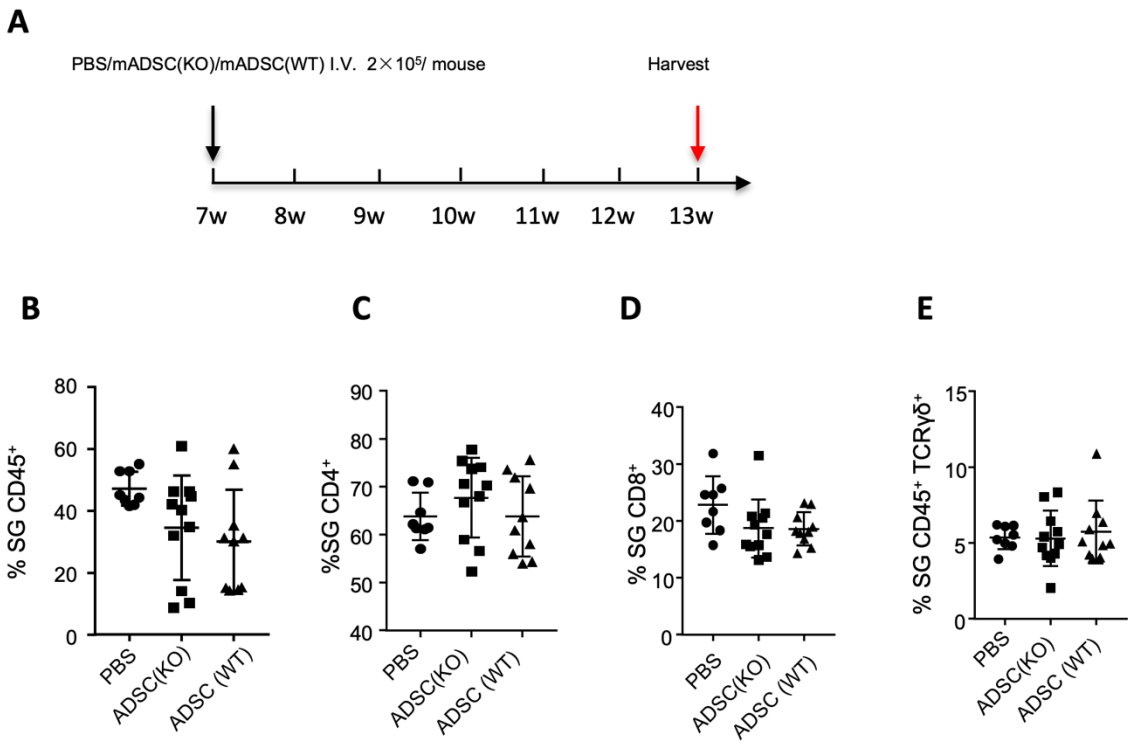

Figure S4. CD45⁺ immune cells express in the submandibular glands of NOD/Ltj mice injected with PBS, ADSC from WT or *Il33*$^{-/-}$ mice. Related to Figure 4.

(A) Experimental workflow of allogeneic mADSCs from WT or il33$^{-/-}$ mice, or PBS infused to NOD/Ltj mice at 7 weeks of age.

(B) Frequency of CD45⁺ cells in the submandibular glands of NOD/Ltj mice injected with PBS, ADSC from WT or *Il33*$^{-/-}$ mice.

(C) Frequency of CD45⁺TCRβ⁺CD4⁺ cells in the submandibular glands of NOD/Ltj mice injected with PBS, ADSC from WT or *Il33*$^{-/-}$ mice.

(D) Frequency of CD45⁺ TCRβ⁺CD8⁺ cells in the submandibular glands of NOD/Ltj mice injected with PBS, ADSC from WT or *Il33*$^{-/-}$ mice.

(E) Frequency of CD45⁺ TCRγδ⁺ cells in the submandibular glands of NOD/Ltj mice injected with PBS, ADSC from WT or *Il33*$^{-/-}$ mice. Data are pooled from three independent experiments. One-way ANOVA was used. Bars, mean; error bars, SEM.

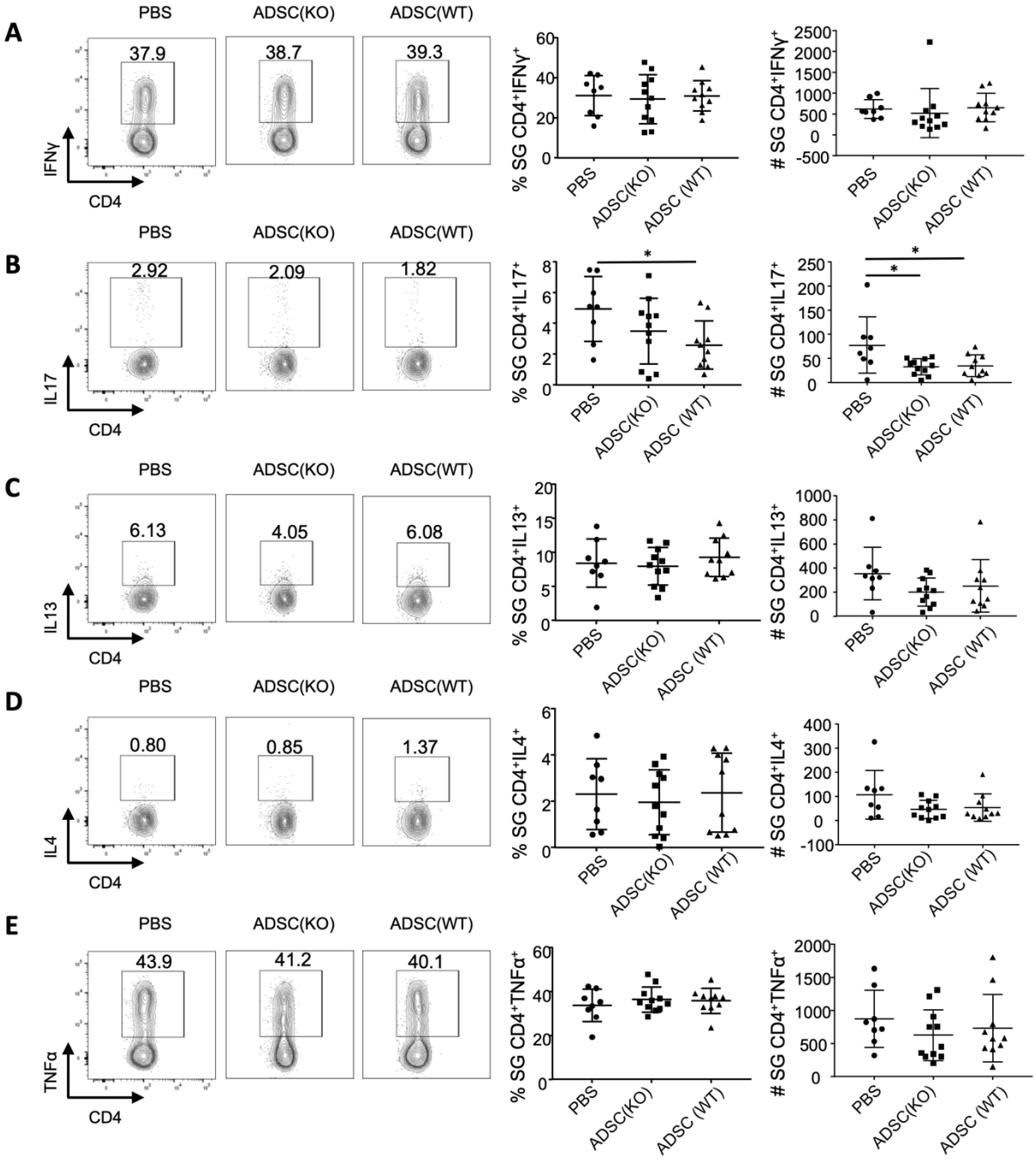
A
PBS
ADSC(KO)
ADSC(WT)
37.9
38.7
39.3
IFNγ
CD4
% SG CD4+IFNγ+
# SG CD4+IFNγ+
B
2.92
2.09
1.82
IL17
CD4
% SG CD4+IL17+
# SG CD4+IL17+
C
6.13
4.05
6.08
IL13
CD4
% SG CD4+IL13+
# SG CD4+IL13+
D
0.80
0.85
1.37
IL4
CD4
% SG CD4+IL4+
# SG CD4+IL4+
E
43.9
41.2
40.1
TNFα
CD4
% SG CD4+TNFα+
# SG CD4+TNFα+

Figure S5. Cytokine expression in TCRβ$^+$CD4$^+$ cells in the submandibular glands of NOD/Ltj mice injected with ADSCs from WT or *Il33*$^{-/-}$ mice. Related to Figure 5.

(A) Frequency and absolute numbers of IFNγ$^+$ in TCRβ$^+$CD4$^+$ cells in the submandibular glands of NOD/Ltj mice injected with PBS, ADSC from WT or *Il33*$^{-/-}$ mice.

(B) Frequency and absolute numbers of IL-17$^+$ in TCRβ$^+$CD4$^+$ cells in the submandibular glands of NOD/Ltj mice injected with PBS, ADSC from WT or *Il33*$^{-/-}$ mice.

(C) Frequency and absolute numbers of IL-13$^+$ in TCRβ$^+$CD4$^+$ cells in the submandibular glands of NOD/Ltj mice injected with PBS, ADSC from WT or *Il33*$^{-/-}$ mice.

(D) Frequency and absolute numbers of IL-4$^+$ in TCRβ$^+$CD4$^+$ cells in the submandibular glands of NOD/Ltj mice injected with PBS, ADSC from WT or *Il33*$^{-/-}$ mice.

(E) Frequency and absolute numbers of TNF-α$^+$ in TCRβ$^+$CD4$^+$ cells in the submandibular glands of NOD/Ltj mice injected with PBS, ADSC from WT or *Il33*$^{-/-}$ mice.

Data are pooled from three independent experiments. One-way ANOVA was used. Bars, mean; error bars, SEM; *P< 0.05.

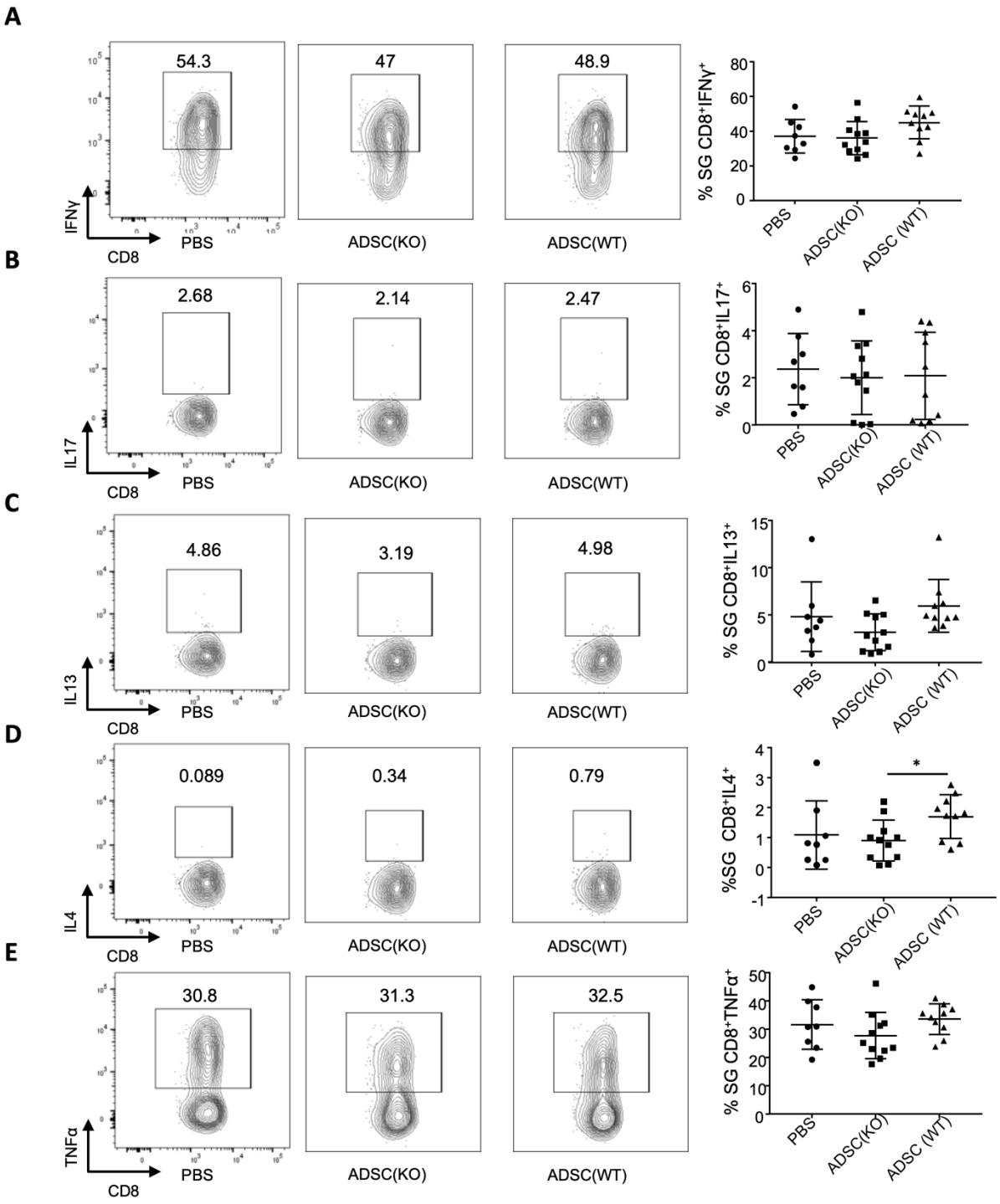
A
54.3
47
48.9
IFNγ
CD8
PBS
ADSC(KO)
ADSC(WT)
% SG CD8+IFNγ+
80
60
40
20
0
PBS
ADSC(KO)
ADSC (WT)
B
2.68
2.14
2.47
IL17
CD8
PBS
ADSC(KO)
ADSC(WT)
% SG CD8+IL17+
6
4
2
0
PBS
ADSC(KO)
ADSC (WT)
C
4.86
3.19
4.98
IL13
CD8
PBS
ADSC(KO)
ADSC(WT)
% SG CD8+IL13+
15
10
5
0
PBS
ADSC(KO)
ADSC (WT)
D
0.089
0.34
0.79
IL4
CD8
PBS
ADSC(KO)
ADSC(WT)
%SG CD8+IL4+
*
4
3
2
1
0
-1
PBS
ADSC(KO)
ADSC (WT)
E
30.8
31.3
32.5
TNFα
CD8
PBS
ADSC(KO)
ADSC(WT)
% SG CD8+TNFα+
50
40
30
20
10
0
PBS
ADSC(KO)
ADSC (WT)

Figure S6. Cytokine expression in TCRβ$^+$CD8$^+$ cells in the submandibular glands of NOD/Ltj mice treated with ADSCs from WT or *Il33*$^{-/-}$ mice. Related to Figure 5.

(A) Frequency of IFNγ$^+$ in TCRβ$^+$CD8$^+$ cells in the submandibular glands of NOD/Ltj mice injected with PBS, ADSC from WT or *Il33*$^{-/-}$ mice.

(B) Frequency of IL17$^+$ in TCRβ$^+$CD8$^+$ cells in the submandibular glands of NOD/Ltj mice injected with PBS, ADSC from WT or *Il33*$^{-/-}$ mice.

(C) Frequency of IL13$^+$ in TCRβ$^+$CD8$^+$ cells in the submandibular glands of NOD/Ltj mice injected with PBS, ADSC from WT or *Il33*$^{-/-}$ mice.

(D) Frequency of IL4$^+$ in TCRβ$^+$CD8$^+$ cells in the submandibular glands of NOD/Ltj mice injected with PBS, ADSC from WT or *Il33*$^{-/-}$ mice.

(E) Frequency TNFα$^+$ in TCRβ$^+$CD8$^+$ cells in the submandibular glands of NOD/Ltj mice injected with PBS, ADSC from WT or *Il33*$^{-/-}$ mice.

Data are pooled from three independent experiments. One-way ANOVA was used. Bars, mean; error bars, SEM; *P< 0.05.

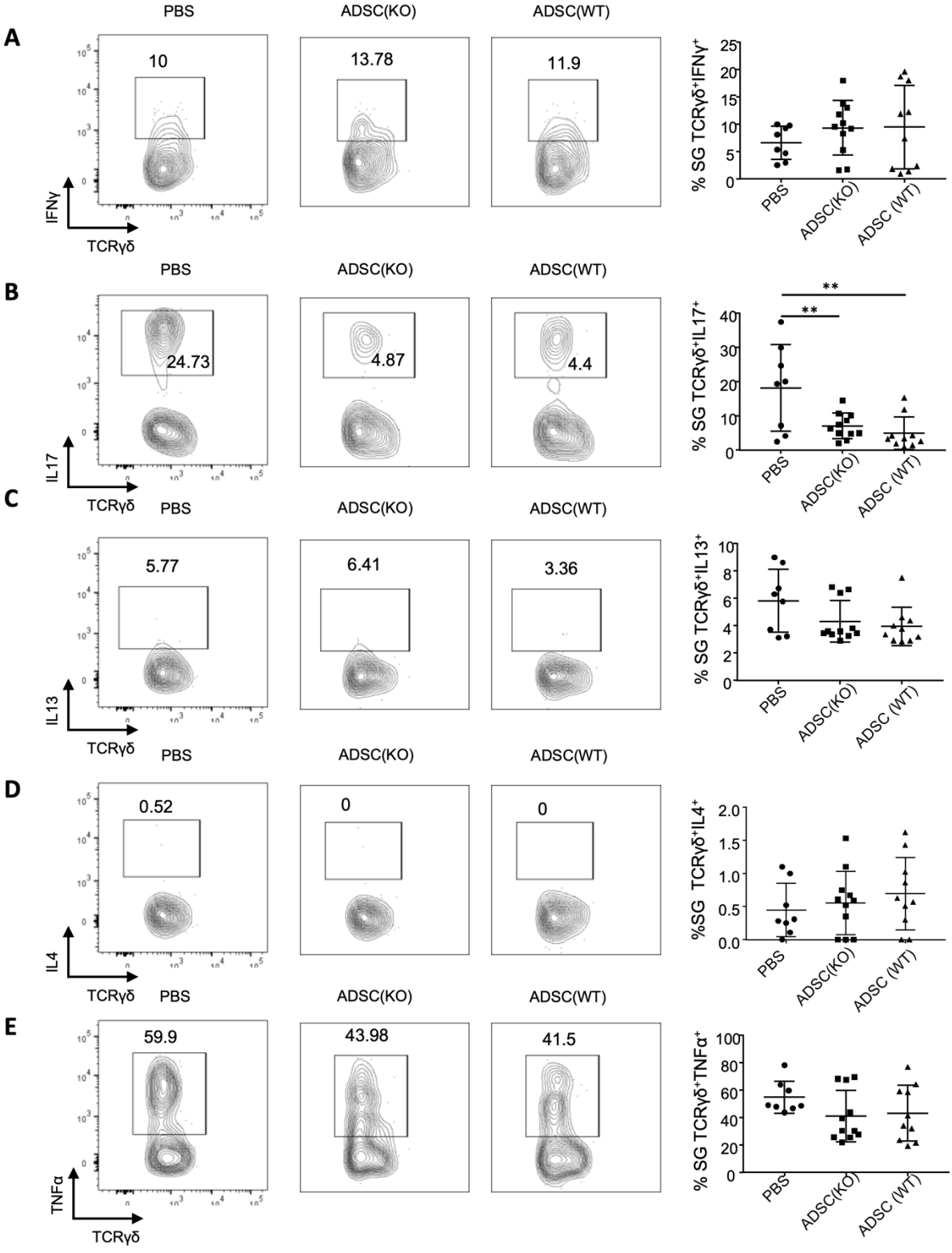
A
PBS
ADSC(KO)
ADSC(WT)
10
13.78
11.9
IFNγ
TCRγδ
% SG TCRγδ+IFNγ+
PBS
ADSC(KO)
ADSC (WT)
B
PBS
ADSC(KO)
ADSC(WT)
24.73
4.87
4.4
IL17
TCRγδ
**
**
% SG TCRγδ+IL17+
PBS
ADSC(KO)
ADSC (WT)
C
PBS
ADSC(KO)
ADSC(WT)
5.77
6.41
3.36
IL13
TCRγδ
% SG TCRγδ+IL13+
PBS
ADSC(KO)
ADSC (WT)
D
PBS
ADSC(KO)
ADSC(WT)
0.52
0
0
IL4
TCRγδ
%SG TCRγδ+IL4+
PBS
ADSC(KO)
ADSC (WT)
E
PBS
ADSC(KO)
ADSC(WT)
59.9
43.98
41.5
TNFα
TCRγδ
% SG TCRγδ+TNFα+
PBS
ADSC(KO)
ADSC (WT)

Figure S7. Cytokine expression in TCRγδ$^+$ cells in the submandibular glands of NOD/Ltj mice treated with ADSCs from WT or *Il33*$^{-/-}$ mice. Related to Figure 5.

(A) Frequency of IFNγ$^+$ in TCRγδ$^+$ cells in the submandibular glands of NOD/Ltj mice injected with PBS, ADSC from WT or *Il33*$^{-/-}$ mice.

(B) Frequency of IL17$^+$ in TCRγδ$^+$ cells in the submandibular glands of NOD/Ltj mice injected with PBS, ADSC from WT or *Il33*$^{-/-}$ mice.

(C) Frequency of IL13$^+$ in TCRγδ$^+$ cells in the submandibular glands of NOD/Ltj mice injected with PBS, ADSC from WT or *Il33*$^{-/-}$ mice.

(D) Frequency of IL4$^+$ in TCRγδ$^+$ cells in the submandibular glands of NOD/Ltj mice injected with PBS, ADSC from WT or *Il33*$^{-/-}$ mice.

(E) Frequency of TNFα$^+$ in TCRγδ$^+$ cells in the submandibular glands of NOD/Ltj mice injected with PBS, ADSC from WT or *Il33*$^{-/-}$ mice. Data are pooled from three independent experiments. One-way ANOVA was used. Bars, mean; error bars, SEM; $^{**}P < 0.01$.

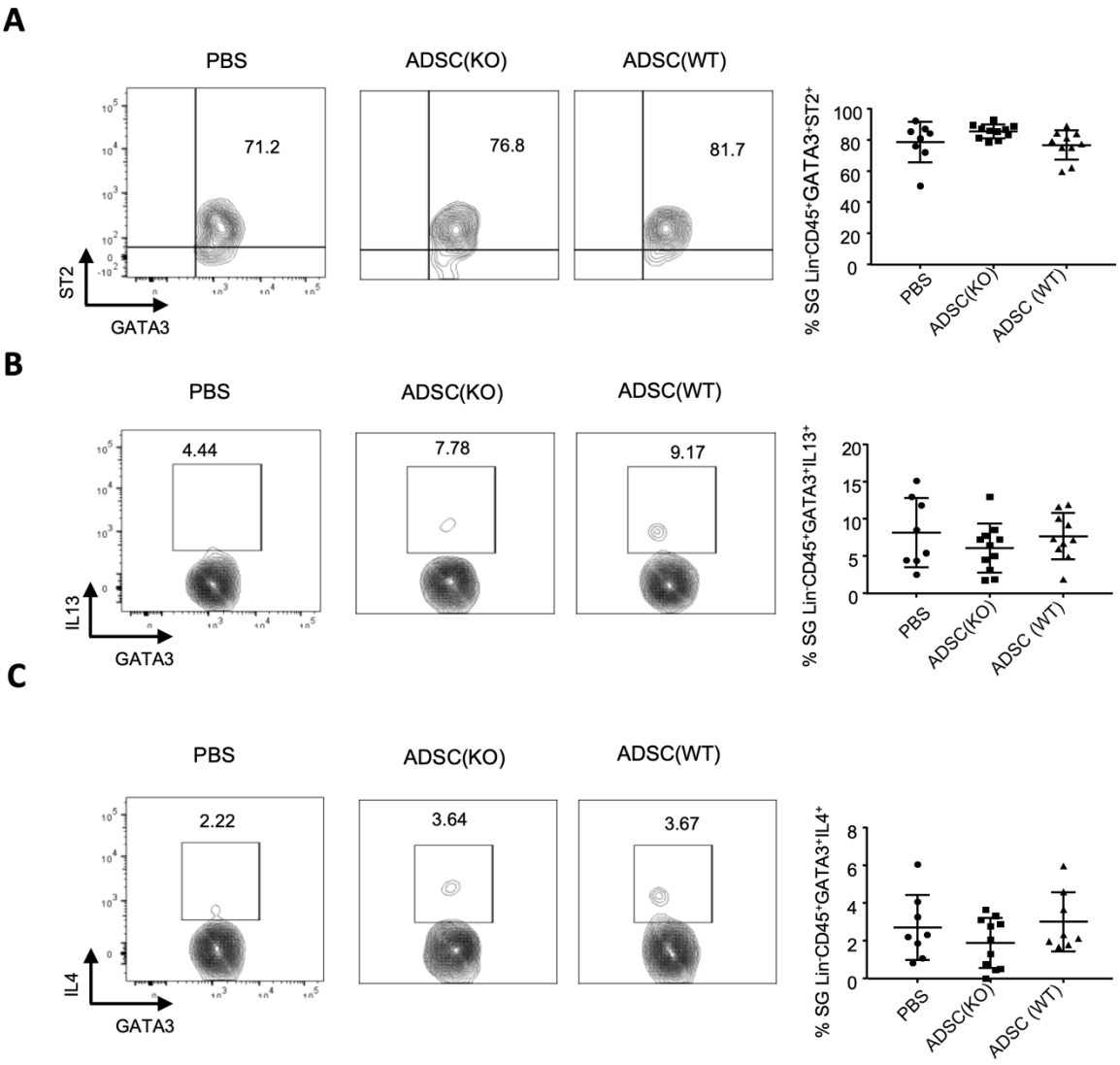

Figure S8. ST2, IL-13, and IL-4 express in ILC2 in the submandibular glands of NOD/Ltj mice injected with ADSCs from WT or *Il33*$^{-/-}$ mice. Related to Figure 5.

(A)The frequency of ST2^{+} in ILC2 in the submandibular glands of NOD/Ltj mice injected with PBS, ADSC from WT or *Il33*$^{-/-}$ mice.

(B) The frequency of IL-13^{+} in ILC2 in the submandibular glands of NOD/Ltj mice injected with PBS, ADSC from WT or *Il33*$^{-/-}$ mice.

(C) The frequency of IL-4^{+} in ILC2 in the submandibular glands of NOD/Ltj mice injected with PBS, ADSC from WT or *Il33*$^{-/-}$ mice.

Data are pooled from three independent experiments. One-way ANOVA was used. Bars, mean; error bars, SEM.

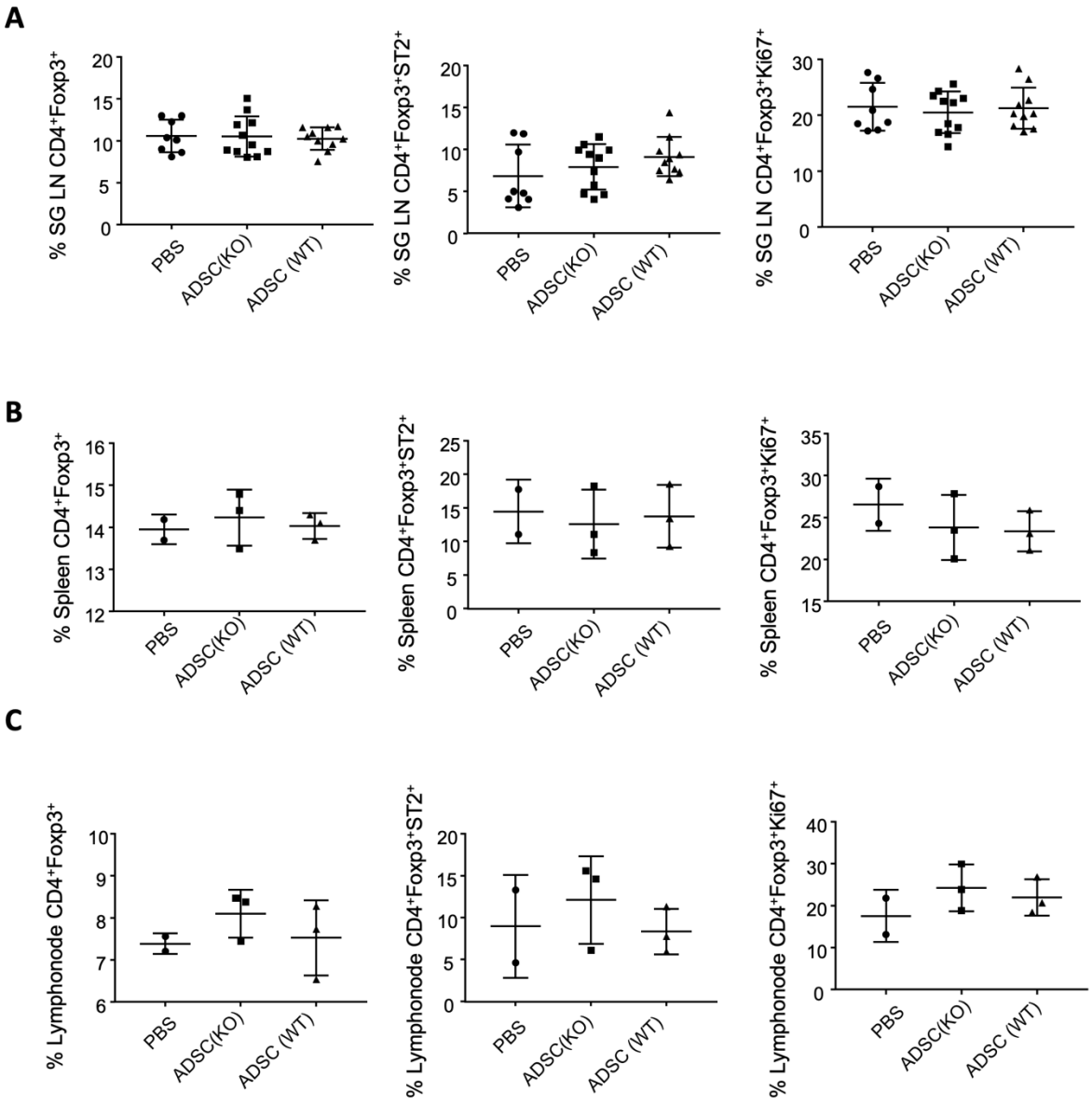

Figure S9. Tregs in the Spleen and lymph nodes of NOD/Ltj mice treated with ADSCs from WT or *Il33*$^{-/-}$ mice. Related to Figure 5.

(A) Frequency of CD4^{+}Foxp3^{+} T, ST2 in Treg and Ki67 in Treg cells in the submandibular lymph node of NOD/Ltj mice injected with PBS, ADSC from WT or *Il33*$^{-/-}$ mice.

(B) Frequency of CD4^{+}Foxp3^{+} T, ST2 in Treg and Ki67 in Treg cells in the spleen of NOD/Ltj mice injected with PBS, ADSC from WT or *Il33*$^{-/-}$ mice.

(C) Frequency of CD4^{+}Foxp3^{+} T, ST2 in Treg and Ki67 in Treg cells in the armpit and inguinal lymph nodes of NOD/Ltj mice injected with PBS, ADSC from WT or *Il33*$^{-/-}$ mice.

Data (A) are pooled from three independent experiments. Data (B and C) are pooled from two independent experiments. One-way ANOVA was used. Bars, mean; error bars, SEM.

Transparent Methods

Mice

Male mice *C57BL/6*, Female NOD/ShiLtj mice *(Cdh23ahl)* mice were purchased from The Jackson Laboratory. Male *mice C57BL/6J- Il33*$^{tm1b(EUCOMM)Cln}$ were donated by Washington University at St. Louis. All animal studies were approved by the Animal Care and Use Committees of National Institute of Dental and Craniofacial Research, National Institutes of Health. 6 to10 weeks old mice were used for all experiments.

Mice/human ADSCs culture

ADSCs were prepared from *C57BL/6* or *C57BL/6J-Il33*$^{tm1b(EUCOMM)Cln}$ subcutaneous fat as described previously[1] and cultured for 2 weeks. Human ADSCs were purchased from Lonza Walkersville Inc, which were isolated from healthy (non-diabetic) adult lipoaspirates collected during elective surgical liposuction procedures. Mice and human ADSCs were cultured in alpha-minimum essential medium containing 20% fetal calf serum and 1% antibiotic-antimycotic (Gibco) in a 5%CO_2 incubator at 37℃. In brief, tissue was minced with two scalpels (crossed blades) and then incubated in a 0.5% collagenase I/phosphate buffered saline (PBS) solution (Collagenase Type: CLS, Biochrom, Berlin, Germany; PBS, Sigma, Taufkirchen, Germany) for 40min at 37°C under constant shaking. The digested tissue solution was then separated through a 100 μm strainer, and the resulting filtrate was centrifuged at 300 g for 5 min. The resulting pellet was washed twice with medium and centrifuged again at 300 g for 5 min. Finally, cells were plated for initial cell culture and cultured at 37°C in an atmosphere of 5% CO_2 in the humid air. alpha-minimum essential medium (α-MEM, Gibco) with a physiologic glucose concentration (100 mg/dL) and used as a standard culture medium. The medium was replaced every three days. Subconfluent cells (90%) were passaged by trypsinization. Cells between passages 2 and 3 were used throughout the experiments. Cell morphology was examined by phase contrast microscopy.

$CD4^+CD25^+$Treg isolation and culture

$CD4^+CD25^+$Tregs from spleen and lymph node from C57BL/6 mice were purified by magnetic cell sorting (Miltenyi Biotec). Tregs were cultured in completed DMEM with or without ADSCs lysates.

ADSCs lysates preparation

ADSCs from WT or *Il33*$^{-/-}$ mice were cultured with IL-1β for 72h. Then ADSCs were broken with ultrasonic method (output power 500W, twice, 5min/each, 4℃) and centrifuged at 14000rpm for 20min.Then the supernatant was collected. $CD4^+CD25^+$Tregs were cultured with IL-1β-stimulated WT or *Il33*$^{-/-}$ ADSC lysates for 24h and 72h with indicated concentration of plate-bound 1μg/ml anti-CD3, 1μg/ml soluble anti-CD28 and 100U/ml IL-2 for 3 days. *Il1rl1* mRNA in Tregs and $ST2^+$Treg were detected by real-time PCR and flow cytometry analysis.

Real-time PCR

Total RNA was derived from cells using RNeasy Mini Kit (QIAGEN) and reversed transcribed using High Capacity cDNA Reverse Transcription Kit (Applied Biosystems). Quantitative real-time PCR was performed according to the protocol of TaqMan Gene Expression Master Mix (Applied Biosystems) with the following TaqMan primers: Hprt, Mm00446968_m1; MmIl33, Mm00505403_m1; MmSt2, Mm00516117_m1; MmCebpα, Mm00514283_s1; MmFabp4, Mm00445878_m1; MmPpar, Mm01184322_m1; MmAlp, Mm00475834_m1; MmSox9, Mm00448840_m1; MmGapdh, Mm99999915_g1; MmFoxp3, Mm00475162_m1; Human Gapdh Hs02758991_m1; Human Il33, Hs04931857_m1.

Western blot analysis

Protein was extracted using RIPA buffer containing proteinase inhibitor cocktail and quantified with a Bio-Rad protein assay. An equal amount of protein was separated on SDS-polyacrylamide gels in a Tris/SDS buffer system and then transferred onto nitrocellulose membranes. Blotting was performed according to standard procedures with primary antibodies against IL-33, ERK, p38, JNK, NF-κB(p65), p-ERK, p-p38, p-JNK, p-NF-κB (p65), β-actin and GAPDH overnight, followed by incubation with appropriate fluorescence-conjugated secondary antibodies. The proteins of interest were analyzed using an Odyssey IR scanner, and signal intensities were quantified using NIH Image/J software.

ELISA assays
To evaluate protein levels of IL-33 in cell lysates and cell culture supernatants, ELISA assays were performed by ELISA kits from R&D Systems according to the manufacturer's instruction.

Flow cytometry analysis
For intracellular cytokine staining, cells were stimulated with PMA (50 ng/ml), Ionomycin (250 ng/ml) and Golgi-Plug (1:1000 dilution, BD PharMingen) at 37℃ for 4h, followed by fixation with the Fixation/Permeabilization buffer solution (BD Biosciences) according to manufacturer's instruction. The staining procedures for MOG38-49-specific tetramer were previously described[2]. Stained cells were analyzed on an LSRFortessa (BD Biosciences), and data were analyzed with FlowJo software.

Allogeneic ADSCs treatment and saliva flow rate measurement
Allogeneic ADSCs from mice *C57BL/6J* or *C57BL/6J-Il33*$^{tm1b(EUCOMM)Cln}$ treatment and saliva flow rate measurement, For ADSCs treatment, NOD/ShiLtj mice were injected with 1*105 ADSCs (from *C57BL/6* or *C57BL/6J-Il33*$^{tm1b(EUCOMM)Cln)}$ in 0.10 ml PBS via the tail vein. Mice were injected with isoproterenol/pilocarpine to stimulate saliva secretion. For saliva flow rate test, mice were weighed, and mild anesthesia was induced with a solution of Ketamine and Xylazine (20 mg/ml; Sigma) in sterile water, given intraperitoneally (1 μl/g of body weight). Salivary secretion was stimulated using 0.1 ml/kg body weight of a pilocarpine solution (50 mg/ml) subcutaneously. Saliva collection began within two minutes of pilocarpine administration. Animals were positioned with a 75-mm hematocrit tube placed in the oral cavity, and the whole saliva was collected into pre-weighed 0.75 ml Eppendorf tubes for 10 minutes. The amount of saliva collected was determined gravimetrically.

Histology
Salivary glands were collected and fixed in 10% formalin (Richard-Allan Scientific), embedded in paraffin, cut longitudinally into 5-mm sections and stained with hematoxylin and eosin. Images were acquired using Aperio digital pathology system and processed in Aperio ImageScope v11.1.2.752 software and the area of inflammatory focus (containing>50 lymphocytes per 4mm^2 tissue) was calculated per field at X200 magnification by Image-Pro Plus Version 6.0 software (Media Cybernetics). Five entire salivary gland sections for each animal were counted with an average of 10 fields by an expert of histopathology under blinded fashion.

Statistics
All data have a normal distribution and are presented as mean ± standard error of the mean (SEM; in data of infiltrating area statistics) or standard deviation (in other data) of three independent experiments, and we used an α level of 0.05 for all statistical tests. The mice salivary flow rates were statistically analyzed with repeated measurement; other data were analyzed with student's t-test, one-way analysis of variance (ANOVA), or two-way ANOVA. All *P* value less than 0.05 were considerate significant. Statistical analysis was done with Graphpad Prism 7.

Regent or Resource source identifier
Antibodies Purified anti-mouse CD3 (145-2C11) Bio X Cell Cat# BE0001-1; RRID: AB_1107634
Purified anti-mouse CD28 (37.51) Bio X Cell Cat# BE0015-1; RRID: AB_1107624
Anti-mouse CD4 Alexa Fluor 405(RM4-5) eBioscience Cat# MCD0426; RRID: AB_1473885
Anti-mouse CD4 Alexa Fluor 700 (RM4-5) eBioscience Cat# 56-0042-82; RRID: AB_494000
Anti-mouse CD4 PerCP-Cy5.5 (RM4-5) eBioscience Cat# 45-0042-82; RRID: AB_1107001
Anti-mouse CD4 PE-Cy7 (RM4-5) eBioscience Cat# 25-0042-82; RRID: AB_469578
Anti-mouse CD8a PerCP-Cy5.5 (53-6.7) eBioscience Cat# 45-0081-82; RRID: AB_1107004
Anti-mouse CD8b FITC (eBioH35-17.2 (H35-17.2)) eBioscience Cat# 11-0083-82; RRID: AB_657764
Anti-mouse CD62L PE (MEL-14) eBioscience Cat# 12-0621-82; RRID: AB_465721
Anti-mouse CD44 APC (IM7) eBioscience Cat# 17-0441-82; RRID: AB_469390
Anti-mouse CD45 Alexa Fluor 700 (30-F11) eBioscience Cat# 56-0451-82; RRID: AB_891454
Anti-mouse CD45 Pacific Blue (30-F11) eBioscience Cat# MCD4528; RRID: AB_1500474
Anti-mouse CD25 PE (PC61.5) eBioscience Cat# 12-0251-82; RRID: AB_465607
Anti-mouse TCRβ APC-Cy7(H57-597) eBioscience Cat# 47-5961-82; RRID: AB_1272173
Anti-mouse TCRγδ Percp-eFlour710 (eBioGL3 (GL-3, GL3)) Cat# 46-5711-82; RRID: AB_2016707

Anti-mouse/rat Foxp3 eFluor 450 (FJK-16a) eBioscience Cat# 48-5773-82; RRID: AB_1518812
Anti-mouse IL-4 PE-Cy7 (11B11) eBioscience Cat# 25-7041-82; RRID: AB_2573520
Anti-mouse IL-10 APC-Cy7 biolegend Cat# 505036; RRID: AB_2566331
Anti-mouse IL-13 PE (eBio13A) eBioscience Cat# 12-7133-82; RRID: AB_763559
Anti-mouse IL-13 PE-eFluor610 (eBio13A) eBioscience Cat# 61-7133-82; RRID: AB_2574654
Anti-mouse IL-17A APC (eBio17B7) eBioscience Cat# 25-7177-82; RRID: AB_10732356
Anti-mouse IFN-γ eFluor 450 (XMG1.2) eBioscience Cat# 48-7311-82; RRID: AB_1834366
Anti-mouse TNF-α PE-ef610 (MP6-XT22) eBioscience Cat# 61-7321-82; RRID: AB_2574666
Anti-mouse-Ki-67 PE-ef610 (SolA15) eBioscience Cat # 61-5698-82; RRID: AB_2574620
Anti-mouse CD3 PerCP-Cyanine5.5 eBioscience Cat # 45-0031-82; RRID: AB_1107000
Anti-mouse Ly-6G/Ly-6C (RB6-8C5), PerCP-Cyanine5.5 eBioscience Cat #45-5931-80; RRID: AB_906247
Anti-mouse CD19 (eBio1D3 (1D3)) PerCP-Cyanine5.5 eBioscience Cat # 45-0193-82; RRID: AB_1106999
Anti-mouse B220 (RA3-6B2) PerCP-Cyanine5.5 eBioscience Cat # 45-0452-82; RRID: AB_1107006
Anti-mouse CD11c (N418) PerCP-Cyanine5.5 eBioscience Cat # 45-0114-82; RRID: AB_925727
Anti-mouse CD11b (M1/70) PerCP-Cyanine5.5 eBioscience Cat # 45-0112-82; RRID: AB_953558
Anti-mouse Fc PerCP-Cyanine5.5 biolegend Cat # 149517; RRID: AB_2632750
Anti-mouse TCRβ (H57-597) PerCP-Cyanine5.5 eBioscience Cat # 45-5961-82; RRID: AB_925763
Anti-mouse NK1.1 (PK136) PerCP-Cyanine5.5 eBioscience Cat # 45-5941-82; RRID: AB_914361
Anti-mouse CD127 (A7R34) Alexa Fluor 700 eBioscience Cat # 56-1271-82; RRID: AB_657611
Anti-mouse Ly-6A/E (Sca-1) (D7) FITC eBioscience Cat # 11-5981-82; RRID: AB_465333
Anti-mouse ST2 (RMST2-2) PE eBioscience Cat # 12-9335-82; RRID: AB_2572708
Anti-mouse ST2 (RMST2-2) Percp-eFluor710 eBioscience Cat # 46-9335-82; RRID: AB_2573883
Anti-mouse GATA3 (RMST2-2) Percp-eFluor710 eBioscience Cat # 46-9335-82; RRID: AB_2573883
Anti-IL-33 antibody [Nessy-1] abcam Cat #ab54385; RRID: AB_881109
P44/42 MAPK(Erk1/2) (L34F12) mouse mAb CST Cat# 4696 ; RRID:AB_390780
Phospho- P44/42 MAPK(Erk1/2) (Thr202/Tyr204) (197G2) Rabbit mAb CST Cat# 4377; RRID:AB_331775
p38 MAPK (D13E1) XP Rabbit mAb CST Cat #8690; RRID:AB_10999090
Phospho-p38 MAPK (Thr180/Tyr182) (28B10) Mouse mAb Cat #9216; RRID:AB_331296
Anti-JNK1+JNK2+JNK3 antibody [EPR16797-211] abcam Cat #ab179461; RRID: AB_2744672
Phospho-SAPK/JNK (Thr183/Tyr185) (81E11) Rabbit mAb Cat #4668; RRID:AB_823588
p65 rabbit mAb (C22B4) CST Cat# 4764; RRID:AB_823578
Phospho-p65 (Ser536) rabbit mAb (93H1) CST Cat# 3033; RRID:AB_331284
GAPDH rabbit mAb (14C10) CST Cat# 2118; RRID:AB_561053

Chemicals, Peptides, and Recombinant Proteins
Recombinant human IL-2 R&D Systems Cat# 202-IL-500
Recombinant human TGF-β1 R&D Systems Cat# 240-B-010
Recombinant mouse IL-1β PeproTech Cat# 211-11B
Recombinant mouse IL-4 PeproTech Cat# 214-14
Recombinant mouse IL-5 PeproTech Cat# 215-15
Recombinant mouse IL-6 PeproTech Cat# 216-16
Recombinant mouse IL-7 PeproTech Cat# 217-17
Recombinant mouse IL-12 PeproTech Cat# 210-12
Recombinant mouse IL-13 PeproTech Cat# 210-13
Recombinant mouse IL-15 PeproTech Cat# 210-15
Recombinant mouse IL-21 R&D Systems Cat# 594-ML-025
Recombinant mouse IL-22 R&D Systems Cat# 582-ML-010
Recombinant mouse IL-23 R&D Systems Cat# 1887-ML-010
Recombinant mouse/rat IL-33 R&D Systems Cat# M3300
Recombinant mouse TNF-α PeproTech Cat# 315-01A
Recombinant mouse IFN-γ PeproTech Cat# 315-05
Recombinant Human IL-1β PeproTech Cat# 200-01B
(5Z)-7-Oxozeaenol R&D Systems Cat# 3604/1
U0126 R&D Systems Cat# 1144/25
SB203580 R&D Systems Cat# 1202/10
SP600125 Invitrogen Cat# tlrl-sp60

JSH23 ab144824 abcam Cat#749886-87-1
PMA Sigma Aldrich Cat# P1585
Ionomycin Sigma Aldrich Cat# I0634
Golgi-Plug BD Biosciences Cat# 555029
TRIzol reagent Invitrogen Cat# 15596026
DNase I Sigma Alcrich Cat# DN25
Collagenase GIBCO Cat# 17104019

Regent or Resource source identifier RNeasy
Mini Kit QIAGEN Cat# 74106
High-Capacity cDNA Reverse Transcription Kit Applied Biosystems Cat# 4368814
TaqMan Gene Expression Master Mix Applied Biosystems Cat# 4369016
Foxp3/Transcription Factor Staining Buffer Set eBioscience Cat# 00-5523-00
Cytofix/Cytoperm Fixation/ Permeabilization Solution Kit BD Biosciences Cat# 554714
$CD4^+$ T cell isolation kit, mouse Miltenyi Biotec Cat # 130-104-456
CD4+CD25+ Regulatory T Cell Isolation Kit, mouse Miltenyi Biotec Cat# 130-091-041

Experimental Models: Cell Lines
hADSC Human Adipose-Derived Stem Cells Catalog #: PT-5006, Lonza Walkersville Inc

Experimental Models: Organisms/Strains
Mouse: C57BL/6 The Jackson Laboratory Cat#000664
Mouse: C57BL/6J-Il33$^{tm1b(EUCOMM)Cln}$ Washington university at St. Louis
Mouse: NOD/ShiLtj The Jackson Laboratory Cat#001976

Oligonucleotides TaqMan
TaqMan Hprt primer, Mm00446968_m1 Applied Biosystems
TaqMan IL33 primer Mm00505403_m1 Applied Biosystems
TaqMan ST2 primer Mm00516117_m1 Applied Biosystems
TaqMan Cebpα, Mm00514283_s1 Applied Biosystems
TaqMan Fabp4, Mm00445878_m1 Applied Biosystems
TaqMan Ppar, Mm01184322_m1 Applied Biosystems
TaqMan Alp, Mm00475834_m1 Applied Biosystems
TaqMan Sox9, Mm00448840_m1 Applied Biosystems
TaqMan Gapdh, Mm99999915_g1 Applied Biosystems
TaqMan Foxp3, Mm00475162_m1 Applied Biosystems
TaqMan Human Gapdh Hs02758991_m1 Applied Biosystems
TaqMan Human Il33, Hs04931857_m1 Applied Biosystems

Regent or Resource source identifier
Software and Algorithms FlowJo 9 software FlowJo, LLC https://www.flowjo.com, RRID:SCR_008520
GraphPad Prism 7 software GraphPad Software https://www.graphpad.com, RRID:SCR_002798
BD LSRFortessa BD Biosciences
BD FACSAria cell sorter BD Biosciences

Supplemental References

1. Gondo S, Okabe T, Tanaka T, Morinaga H, Nomura M, Takayanagi R, et al. Adipose tissue-derived and bone marrow-derived mesenchymal cells develop into different lineage of steroidogenic cells by forced expression of steroidogenic factor 1. Endocrinology. 2008;149(9):4717-25.
2. Kasagi S, Zhang P, Che L, Abbatiello B, Maruyama T, Nakatsukasa H, et al. In vivo-generated antigen-specific regulatory T cells treat autoimmunity without compromising antibacterial immune response. Science translational medicine. 2014;6(241):241ra78.